LAMINAR BOUNDARY LAYERS IN THE NEIGHBORHOOD OF ABRUPT SPATIAL DISTURBANCES

Thesis by

Thomas Janney Tyson

In Partial Fulfillment of the Requirements

For the Degree of

Doctor of Philosophy

California Institute of Technology

Pasadena, California

1967

(Submitted May 16, 1967)

This work is dedicated to the memory of my father,

Howell N. Tyson, Sr.

ACKNOWLEDGMENTS

Many have contributed toward my education at the California Institute in both a personal and a technical way. To all of these individuals I wish to express my gratitude.

To the family of the late Dr. Clark B. Millikan, I would like to acknowledge my feelings of respect and indebtedness. His unbounded enthusiasm and energies devoted to GALCIT and its students, have been reflected in many graduates of the past. One hopes to see this spirit preserved.

I also wish to thank Dr. Ernest Sechler for his encouragement; Professors Toshi Kubota and Lester Lees for their interest and technical guidance. Mrs. Truus van Harreveld deserves special thanks for her competent assistance with the figures and computations.

I wish to acknowledge, with much appreciation, the financial support provided me by the California Institute throughout my graduate work and by the Ford Foundation for the academic year 1966 - 1967.

Finally, I would like to acknowledge the encouragement given to me by all of my family. To my wife Joanne in particular, thank you.

ABSTRACT

Supersonic, steady laminar boundary layers exhibiting "strong" local interaction with the outer flow are considered. The general behavior of such flows on a flat adiabatic plate are studied by means of the "moment method" equations and by finite difference solutions of the full boundary layer equations, including the transverse momentum equation. A one-parameter family of "free interaction" solutions is generated with the finite difference approach. These include separated reverse flow solutions. The infinite plate solution is established from the leading edge through weak interaction by both techniques. Expansive corner flow solutions are developed using both methods. In the "moment method" study the nature of the leading edge, Blasius point and "critical" line singularities is developed by numerical investigation.

TABLE OF CONTENTS

TABLE OF CONTENTS (Cont'd)

TABLE OF CONTENTS (Cont'd)

TABLE OF CONTENTS (Cont'd)

LIST OF FIGURES

LIST OF SYMBOLS

D, N_1, N_2, N_3, $\mathcal{K}$, P, J, R, Z, B, h, β, f, ξ are defined in Appendix 1 and equations 3.1 in accordance with the moment method formulation.

A	stream tube area
a	velocity profile parameter (see Appendix 1); speed of sound
C_∞	$(\mu/\mu_\infty)/(T/T_\infty)$
c_p	specific heat at constant pressure
$F(\eta)$	coordinate transformation function
h	step size in x-direction; moment method function
j	iteration number; axisymmetry parameter
K	inverse characteristic length for "departure"
L	arbitrary length scale; plate length; "departure" length
m	$(\frac{\gamma-1}{2})\, M^2$
M	Mach number
$\bar{M}$	"mean" Mach number across boundary layer
n	natural coordinate normal to streamlines; exponent in coordinate transformation
P	pressure
P_1	"base" pressure in Lighthill linearization
P_{WI}	"weak interaction" pressure
R	streamline radius of curvature; wall radius of curvature
Re	$\frac{\rho_\infty U_\infty L}{\nu_\infty}$, $\frac{\rho_\infty U_\infty x}{\nu_\infty}$
$\tilde{R}e_{\delta_i^*}$	$\frac{a_\infty M_e \delta_i^*}{\nu_\infty}$
$Re_{\delta_i^*}$	$\frac{a_\infty M_\infty \delta_i^*}{\nu_\infty}$

S	$\Delta\eta$ the lateral mesh spacing
T	temperature
U	velocity in the streamwise coordinate direction
V	velocity in the normal coordinate direction
x	distance along surface coordinate
y	distance normal to surface
Y	distance normal to surface in transformed (Stewartson) coordinates
α_w	wall inclination angle
γ	ratio of specific heats c_p/c_v
δ	boundary layer thickness
δ_i	transformed boundary layer thickness
δ_i^*	transformed displacement thickness
η	transformed lateral coordinate = $F(y/x^n)$
θ	outer edge inclination angle; wall inclination angle; momentum thickness
θ_i	transformed momentum thickness
$\varkappa$	wall curvature
λ	ratio of adjacent streamwise step sizes
μ	viscosity
ν	μ/ρ
$\nu(M)$	Prandtl-Meyer angle
ξ	P_e/P_∞
ρ	density

Subscripts

B	Blasius
e	local "edge" value
i	transformed variable
w	wall condition
$\infty, \infty-$	undisturbed free stream values, upstream
$\infty+$	asymptotic values at downstream infinity
c	corner location

1. INTRODUCTION

This investigation is directed toward the study of supersonic, steady, laminar boundary layer mechanics. The emphasis is placed on those situations for which there is a strong coupling between the outer and boundary layer flows. This coupling is characterized by the fact that the "induced" pressure in the outer flow, due to the presence of the boundary layer, is of such a magnitude that it has an effect on the dominant boundary layer behavior. Hence the development of both the outer and boundary layer solutions must be carried out simultaneously. Such "strong local interaction" will be initiated, for example, when the boundary layer approaches a compression or expansion corner.

Particular attention is placed on the so called "free interactions". The name stems from the fact that for this class of interaction phenomena, the boundary layer responds to a stimulus which is entirely a consequence of the upstream propagation from some downstream disturbance. No wall induced disturbance or impinging disturbance waves from the outside are present. These are the "upstream influence" solutions.

"Interaction" between the boundary layer and outer flow is, of course, always present to some extent. It can be categorized both by the degree to which it is present and by the manner in which it enters the mathematical formulations. If the dominant boundary layer behavior can be established by consideration of a known outer flow solution in the absence of a viscous layer, then the interaction is said to be "weak".

There is another important class of strong interaction solutions for which, again, there are no locally impinging waves from the outside and no local disturbances emanating from the wall. These correspond to those situations in which the boundary layer, having experienced and passed through a zone of disturbance, relaxes back into a weak interaction regime, e.g. toward the Blasius solution on an adiabatic flat plate.

One distinguishing feature of strong interaction phenomena is the attendant short characteristic length relative to that for "weak" interaction. Thus, as one would expect, abrupt physical disturbances will generate this type of behavior. In addition, and especially for expansive interaction, there can be a first order effect due to the presence of lateral pressure gradients.

The general features of interaction phenomena were first investigated using the "moment method" as developed by Lees and Reeves (1). This formulation allows great simplification of the governing equations, but with an attendant reduction in information content of the variables describing the layer. The method and the numerical investigation are presented in Section 3. The general mathematical behavior of the solutions for this formulation was obtained by numerical experimentation. In addition, an expansive corner flow was investigated using the moment method technique.

In Section 4 the full partial differential equations appropriate to interacting boundary layers are numerically integrated. These equations differ from the usual Prandtl formulation primarily in the inclusion of the lateral pressure gradient in addition to the interaction coupling. Free interactions and corner flow solutions are presented. In conjunction with the latter, separation behavior is obtained.

The primary goal for the finite difference study of Section 4 is to establish the feasibility of such an approach and to set forth some tentative guide lines for its implementation.

Section 2 introduces the general subject by means of a brief discussion of order of magnitude considerations and a review of Lighthill's (2) treatment of the linearized interaction problem.

2. PRELIMINARY CONSIDERATIONS

2.1. General

The primary emphasis in this investigation has been on the "moment method" and the finite difference representation of the boundary layer field equations. However, before embarking on those aspects of the study, it is worthwhile to establish a few qualitative ideas about such boundary layer behavior.

2.2. Order Of Magnitude Estimates

Consider a boundary layer of height δ expanding over a corner located a distance L from the leading edge of a flat plate. See Figure 1 for a schematic. It is possible with simple order of magnitude arguments, and a little foreknowledge of the actual behavior, to conjecture with some confidence about the general behavior in various regions. First of all, consider a region adjacent to the wall of the order of a boundary layer thickness in lateral extent, and assume that $\frac{\Delta P}{P_\infty}$ within this region is O(1). (Computational and experimental evidence confirm this for all but very small angles). Then it can be shown from the Navier-Stokes equations that three possible distinguished limits exist, depending upon the order of the character-

istic length in the x-direction. If the x-characteristic length is the order of L then we recover the usual Prandtl boundary layer formulation. If it is intermediate between L and δ , the limit corresponds to the inviscid Prandtl equations; that is, the flow is inviscid but cannot support a lateral pressure gradient. And finally, if the x-length is $O(\delta)$, the governing equations are fully inviscid and an O(1) lateral pressure gradient exists. Again, we know from experimental and computational evidence that a substantial lateral pressure gradient can indeed exist at the corner and the observed characteristic length is $O(\delta)$. Then to conclude, we note the need for still another limit near the wall for which viscous forces are comparable to inertia terms. Such a limit will thus be able to handle the no-slip boundary condition.

The limit sought, for which $\frac{\Delta P}{P_\infty} = O(1)$ and viscous terms are comparable to inertia terms, has a Prandtl-like behavior. This viscous sublayer is of $O(\delta^{\frac{3}{2}})$ in lateral extent.

The schematic of Figure 1 evolved from the consideration of these several limits. It shows, in addition, a very small Stokes-like region right at the corner.

It should perhaps be emphasized at this point that in

referring to an "inviscid" region, it does not imply the vanishing of viscous stresses. Indeed, shearing stresses exist to the same order as in the fully Prandtl-like layer upstream. The implication of an "inviscid" distinguished limit is that the dominant behavior of the perturbation quantities is inviscid. The flow, of course, achieved its general vortical nature through the action of viscosity upstream.

2.3. The Inviscid Interaction Model

On the basis of the above arguments, suppose for the moment that a laminar boundary layer responds to a downstream disturbance in a completely inviscid manner. Suppose further, that the region under consideration is sufficiently far upstream that the lateral pressure gradient vanishes. The one-dimensional isentropic pressure-area relation for a stream tube is

$$\frac{dP}{P} = \gamma \left(\frac{M^2}{1-M^2} \right) \frac{dA}{A}$$

Let η be the streamline inclination. Then, linearizing the above relation about a base Mach number profile $M(y)$ and pressure P_1, we obtain

$$\frac{\partial P}{\partial x} = \gamma P_1 \frac{M^2(y)}{1 - M^2(y)} \frac{\partial \eta}{\partial y} \qquad (2.1)$$

Integration gives

$$\theta = \frac{1}{\gamma P_1} \frac{dP}{dx} \int_0^{\delta} \left(\frac{1 - M^2(y)}{M^2(y)} \right) dy$$

where θ is the "edge" inclination at $y = \delta$. The integral diverges if $M(y) \sim y$ near $y = 0$. For this approach to be meaningful, an "effective" $M(0)$ must be established from considerations of the inner viscous sublayer.

Now, using the Prandtl-Meyer relation at the edge, we have

$$\theta = \frac{1}{K} \frac{d\theta}{dx}$$

where

$$(K)^{-1} = \frac{M_e^2}{(M_e^2 - 1)^{\frac{1}{2}}} \int_0^{\delta} \left(\frac{1 - M^2(y)}{M^2(y)} \right) dy$$

Hence

$$\theta = C \exp \left[K(x - x_o) \right]$$

or, defining a mean Mach number by

$$\bar{M} = \left(\int_0^1 \frac{1}{M^2(\frac{y}{\delta})} \, d(\frac{y}{\delta}) \right)^{-\frac{1}{2}}$$

gives

$$\theta = C \exp \left[\frac{M_e^2}{(M_e^2 - 1)^{\frac{1}{2}}} \cdot \left(\frac{1 - \bar{M}^2}{\bar{M}^2} \right) \left(\frac{x - x_o}{\delta} \right) \right]$$

Thus for the boundary layer to be able to respond with positive exponential solutions, the mean Mach number must be

subsonic. There is a direct correspondence between this and the subcritical-supercritical distinction made in the moment method formulation.

2.4. Lighthill's Approach

Lighthill (2) treats the problem of supersonic boundary layers subject to weak disturbance imposed either at the wall or from outside the boundary layer. He linearizes what appear to be appropriate limits of the Navier-Stokes equations and numerically patches the solutions in such a manner as to give a hopefully valid solution throughout the regions of interest. He argues, in effect, that the perturbation quantities, associated with a local disturbance, will have a sufficiently short characteristic length to be governed by the inviscid perturbation equations. The exception to this is a very thin sublayer near the wall where viscous effects must be retained in order to satisfy the no-slip condition. The argument thus parallels that of 2.2 except that the perturbations here are of smaller order.

In addition to equation (2.1) in 2.3 above, Lighthill introduces the lateral momentum equation

$$\frac{\partial P}{\partial n} = -\frac{\rho u^2}{R}$$

where "n" is the normal coordinate and R is the streamline radius of curvature. Linearizing, we have

$$\frac{\partial P}{\partial y} = -\gamma P_1 M^2(y) \frac{\partial \eta}{\partial x} \qquad (2.2)$$

Solving this set of equations for the upstream influence length $(K)^{-1}$, he obtained

$$(K)^{-1} = \frac{M_e^2}{(M_e^2-1)^{\frac{1}{2}}} \left[\int_0^\delta \left(\frac{1-M^2(y)}{M^2(y)} \right) dy + \left(\frac{M_e^2-1}{M_e^4} \right) \int_0^\delta M^2(y) dy \right]$$

The deviation between this and the result obtained in 2.3. is in the second term. Its presence eliminates the arbitrariness associated with defining an "edge" location. Notice that the contribution of the integrals in the outer region cancel.

Lighthill goes on to point out that this result is only descriptive at best without a knowledge of the appropriate value of M(0), the wall-side boundary condition for the inviscid flow. In order to establish this value, he linearizes the Navier-Stokes equations about the upstream undisturbed linear velocity distribution near the wall. This results in the time independent Orr-Sommerfeld equation. Matching of the inner and outer regions is accomp-

lished by matching the respective Fourier transformations of the solutions.

Lighthill's estimate, using this approach, of the appropriate wall-side Mach number for a laminar layer on a flat plate is

$$M(0) = 0.63\,(\bar{\chi})^{\frac{1}{4}}$$

where $\bar{\chi}$ is the interaction parameter $M_{\infty}^{3}/(Re_{x})^{\frac{1}{2}}$.

Comparison of this estimate of upstream influence with a moment method estimate is given in Section 3.3.3.

The major assumptions of Lighthill's approach are that 1) the sublayer is incompressible; 2) the "base" profile in the sublayer is linear; and 3) his method of matching the solutions is valid. He shows by an a posteriori check that all of his assumptions are self consistant with his results.

3. MOMENT METHODS

3.1. General Remarks

The "moment method" technique has been utilized in this section to study the general nature of laminar boundary layer interaction on a flat plate. For general background information on the method, derivation of the equations, discussion of the critical point and application the reader is referred to Lees and Reeves (1).

In the course of this investigation the infinite flat plate solution is obtained starting at the leading edge. The solution so obtained is one of a one-parameter family of solutions that represent all solutions which eventually decay to the Blasius solution downstream. The question of analyzing expansive corner flows is then pursued. This raises the question of the existence of solutions which pass smoothly through the "critical point" from supercritical to subcritical. It is found that indeed such solutions exist.

3.2. The Differential Equations

In the moment method of Lees and Reeves (1), the boundary layer is completely described by three variables; the

outer edge Mach number and two velocity profile parameters, "a" which is directly related to the wall shear and δ_i^* which is a measure of the displacement thickness. If δ_i^* and x are normalized with respect to $\left(\frac{\nu_\infty}{a_\infty M_\infty}\right)$, then a single parameter M_∞ enters the equations for flat plate flow; if the wall is curved the wall curvature distribution, normalized in the same manner, also enters the description. All other quantities such as physical boundary layer height, wall shear, etc. can be determined by auxiliary calculation in terms of the variables and parameters mentioned.

The principal assumptions of the method are: 1) the family of velocity profiles can be adequately described by a single shape parameter, 2) the lateral pressure gradient can be assumed zero, 3) an appropriate choice of the boundary layer "edge" definition can be made, and 4) the particular choice of governing equations is satisfactory. Assumptions 2) and 3) are directly related and common to Prandtl type boundary layer analysis in any form, not just the moment method approach. Each of these assumptions will be discussed later. The equations in their most convenient form for numerical treatment are:

$$\frac{\delta_i^*}{M_e}\frac{dM_e}{dx} = \frac{\beta C}{\bar{R}e_{\delta_i^*}}\frac{N_1(M_e, a, h)}{D(M_e, a)}$$

$$\delta_i^*\frac{d\aleph}{dx} = \frac{\beta C}{\bar{R}e_{\delta_i^*}}\frac{N_2(M_e, a, h)}{D(M_e, a)} \qquad (3.1)$$

$$\frac{d\delta_i^*}{dx} = \frac{\beta C}{\bar{R}e_{\delta_i^*}}\frac{N_3(M_e, a, h)}{D(M_e, a)}$$

where

$$N_1(M_e, a, h) = \left(J - \aleph\frac{dJ}{d\aleph}\right)h + (\aleph R - PJ) + \left(P\frac{dJ}{d\aleph} - R\right)B$$

$$N_2(M_e, a, h) = J(\aleph - 1)h + (PJ - \aleph R)f + [(2\aleph+1)R - 3JP]B$$

$$N_3(M_e, a, h) = \left[(2\aleph+1)\frac{dJ}{d\aleph} - 3J\right]h + \left(R - P\frac{dJ}{d\aleph}\right)f + \left[3JP - (2\aleph+1)R\right]$$

$$D(M_e, a) = \left(J - \aleph\frac{dJ}{d\aleph}\right)f + (\aleph - 1)J + \left[(2\aleph+1)\frac{dJ}{d\aleph} - 3J\right]B$$

The variables $\aleph$, J, P, R and Z are functions of "a" alone, the specific functional dependence depending on the profile family that has been selected. In the derivation of the equations, a Howarth transformation was applied so that the Falkner-Skan similitude solutions could be effectively adopted as the one-parameter family. Klineberg (3) has obtained the above functions of "a" corresponding to this family. These relations, along with additional definitions for other functions appearing in the equations, are given in Appendix 1. The interaction equation relating

the streamline inclination at the outer edge to the pressure is taken either as the Prandtl-Meyer or tangent-wedge relation. These are also given in Appendix 1.

3.3. Some Preliminary Analytical Considerations

3.3.1. The Singularities

3.3.1.1. The Leading Edge

The leading edge is an isolated node-saddle singularity in the three-dimensional phase space M, a, $Re_{\delta_i}{}^*$. The tangent-wedge interaction equation is employed along with the hypersonic approximation for the isentropic pressure-Mach number relation in the neighborhood of this point. The singularity is characterized by the simultaneous vanishing of $Re_{\delta_i}{}^*$, M, and N_2. The general character can be established by the linearization method of Poincaré, but the only solution of physical interest is the exceptional path passing through the point tangent to all the nodal solutions. The behavior of this solution can be obtained by an algebraic coordinate expansion in small x. This was done by Lees (4) who showed that the appropriate expansion is in large $\bar{\chi}$ where $\bar{\chi} = \frac{M_\infty{}^3\sqrt{C_\infty}}{\sqrt{Re_x}}$. The expansion describes the exceptional trajectory quite well down to a $\bar{\chi}$ of 5 or so. The other nodal solutions

are not represented because of their exponential nature near the singular point.

Klineberg (3) has carried the leading-edge expansion to third order and this expansion has been compared to the numerical solutions obtained in this study. The expansion is given in Appendix 2.

3.3.1.2. The "Blasius" Point and The "Relaxation" Surface

The Blasius point will be defined as the point $\delta_i^* = \infty$, $a = a_B$, $M_e = M_\infty$ in the phase space. A one-parameter family of solutions, forming a surface in the phase space, relaxes to this point. The behavior of N_1, N_2, N_3 and D near the Blasius point cannot be described by a linear approximation and hence an analytical study would be very difficult. An asymptotic coordinate expansion for large x can be obtained - the so called "weak interaction" expansion. Again, the appropriate expansion variable is $\bar{\chi}$. Such an expansion has recently been carried out with retention of third order terms by Klineberg (3). His results are given in Appendix 2. This expansion has been used in this study for comparison against numerical results. Such an expansion has the same limitations as mentioned for the small-x coordinate expansion at the leading

edge. It cannot describe the general nature of the singularity, but only the common asymptotic nature of the integral paths going into the singular point.

The nature of the solution curves in the neighborhood of this point have been found by numerical investigation. A general description follows of the integral paths which go to Blasius. The justification for these conclusions and the method of establishing them will be presented later.

Figures 3 and 4 show integral paths in the M-a, $Re_{\delta_i}{}^*$ - a planes respectively. There is a one-to-one correspondence between the curves in the two Figures. The surface generated by these integral paths can be appropriately called the "relaxation" surface, for all integrals which do relax to the Blasius point lie in this surface. Figure 2 gives a rough schematic of a portion of this surface. The level lines are indicated by light lines, the integral paths by heavy lines. Figure 5 shows level curves in the M-a plane for constant values of $Re_{\delta_i}{}^*$.

Consider the integral curves in the surface for large $Re_{\delta_i}{}^*$ for which the deviation of M and "a" from the Blasius values is small. The infinite plate solution is one such curve and the others can be envisioned as "perturbed" infinite plate solutions, i.e. infinite plate solutions

which have experienced a perturbation due to some "external" disturbance such as wall blowing or an incident wave impinging on the layer. Such solutions are precisely those sought by Libby and Fox (5) in their treatment of the full boundary layer equations. Their analysis ignores the weak interaction coupling with the outer flow and the question then arises as to whether this is a valid omission. The momentum and moment of momentum equations can be used to establish $a(x)$ and $Re_{\delta_i}^*(x)$ in the absence of interaction, i.e. under the constraint that M_e is constant. However, an examination of the equations indicates that if $\frac{dM}{da}$ is larger than about .03, interaction coupling is significant. Now it is not clear from Figure 5 what the asymptotic value of $\frac{dM}{da}$ is for the surface solutions as $Re_{\delta_i}^*$ goes to infinity. If $\frac{dM}{da}$ goes to some finite limit greater than .03 as $Re_{\delta_i}^*$ goes to infinity, then the Libby-Fox treatment is not valid for hypersonic flows even in the large $Re_{\delta_i}^*$ limit, and one must include the weak interaction terms. A few more calculations should be made to define this portion of the surface and resolve the question.

Relaxing boundary layers characterized by points lying on the surface well removed from the Blasius point, can descriptively be referred to as strong interaction

relaxation solutions. Examples would be the relaxation to Blasius following a shock induced separation or following a rapid expansion around a corner.

The "relaxation" surface also contains a line of singularities, the "critical line", to be discussed in the next section. All points in the surface on the Blasius point side of the critical line are the so called "subcritical" points. On this "subcritical" side, all points not on the surface lie on integral paths which diverge from it as x increases. On the opposite or "supercritical" side, the integral curves which pass through the critical line into the subcritical surface do not form a single surface. However, these paths do relax to a well defined surface which is a continuous extension of the subcritical "relaxation" surface. The distinction here is that while on the subcritical side the paths diverge from the surface, on the supercritical side they converge toward a surface as x increases. With this distinction in mind, it is conceptually helpful to consider a single relaxation surface spanning the critical line.

If an appropriate interaction equation is used such as the tangent-wedge relation, then the surface also contains the leading edge singularity and hence the complete

semi-infinite plate integral curve.

The "departure" integrals will be defined as those paths diverging from the subcritical relaxation surface. An integral path which is close to the relaxation surface at some point does not remain close. In general, it has a characteristic length for departure which is much smaller than the local characteristic length of curves in the surface. Again, integral paths near the relaxation surface on the supercritical side do not depart from it but rather decay toward it.

3.3.1.3. The "Critical Line"

Referring again to equations (3.1), the "critical line" is a line of singularities in the phase space associated with the simultaneous vanishing of D, N_1, N_2 and N_3. When D=0, the vanishing of any one of the N's implies the vanishing of the other two, hence the locus of critical points is a line. This is a consequence of the fact that the N's and D are not unrelated, but result from inverting a set of equations of the form

$$\vec{A}\dot{\vec{y}} = \vec{b}$$

The Poincaré method of analyzing singular point behavior may fail to fully describe the behavior in the

neighborhood of a line singularity. Functions N_1, N_2 and N_3 are regular with dominant linear behavior and generally well behaved in the neighborhood of the critical line. However, it has been shown by Poincaré and Liapunov (6) that the above behavior in itself is not sufficient to guarantee that the linearized system of equations will have solutions representative of the nonlinear system. In order to guarantee that nonlinear effects will be negligible, the linear system must have neither a zero eigenvalue nor a pair of pure imaginary complex conjugate eigenvalues. The latter case often occurs with isolated singularities associated with dynamical systems. The eigenvalues cited correspond to a center-type singularity, i.e. a periodic motion, whereas the nonlinear system may well possess a spiral-type behavior with the paths driving into or out of the origin.

Any system with a line of singularities possesses a zero eigenvalue with the associated eigenvector tangent to that line; i.e., in this direction the linearized functions N_1, N_2, N_3 and D all remain zero. The writer has carried out the linear analysis of this singular behavior without success.

Physical intuition, on the other hand, leads one to expect smooth relaxation from highly expanded states to the Blasius point. Further, one feels that the fundamental moment method assumptions are probably not seriously violated in those physical situations which exhibit such "smooth" behavior. Hence a numerical investigation of the critical line was undertaken.

The picture resulting from the numerical investigation is as follows. The singularity has a nodal character. The nodal paths represent solutions passing smoothly through the critical line from supercritical to subcritical with increasing x. There is an exceptional nodal path which lies in the relaxation surface whereas all other node paths converge towards it on the supercritical side and diverge from it on the subcritical side. The nodal paths at the critical line are characterized by increasing M and $Re_{\delta_i}^*$ and decreasing "a".

3.3.2. The "Departure" Solutions

Integrating forward in x, all integral paths initially near the subcritical relaxation surface "depart" from it; and in general their characteristic length is much smaller than for curves in the surface itself. For any

point on the surface this departure length can be determined by linearizing the equations about the known solution on the surface and seeking the solutions which lie close to but not on the surface. If one further invokes the "departure" characteristic that the perturbation derivatives will be much larger than the surface solution derivatives, one obtains a linear system with a single eigenvalue, namely that one associated with rapid divergence from the surface. The eigen solutions associated with integrals in the surface itself are suppressed. This simplification can not be made near the leading edge singularity where the large surface derivatives must also be retained in order to adequately describe the departure. Kubota (7) carried out such a linearization for the weak interaction regime. The results he obtained are general, however, and should apply over a major portion of the surface with the exception of regions near the leading edge. From Kubota's analysis, which invoked the hypersonic limit, one can deduce that the characteristic departure length L is given by

$$\frac{L}{\delta_i^*} = \left(\frac{\gamma-1}{2}\right)^2 M_\infty^3 \left(\frac{M_e}{M_\infty}\right)^{\frac{3\gamma-1}{\gamma-1}} \cdot \left[\frac{\frac{dJ}{d\aleph} - J - (\aleph \frac{dJ}{d\aleph} - J)\left(\frac{2}{\gamma-1} + \frac{\gamma+1}{\gamma-1}\aleph\right)}{\aleph J - J}\right] \quad (3.2)$$

(If required, the hypersonic restriction can be removed without difficulty.) If the weak interaction expansion is used, we obtain

$$\frac{L}{x} = 7.6\left(\frac{\gamma-1}{2}\right)^3 \bar{\chi} \tag{3.3}$$

or

$$\frac{L}{\delta} = 3.22\left(\frac{\gamma-1}{2}\right) M_\infty$$

where x is the length from the leading edge and δ is the physical boundary layer height.

If the strong interaction expansion is used, one might expect the procedure to fail since the surface derivatives are also going to infinity. Nevertheless, it probably gives the qualitatively correct picture of how the L/δ ratio varies as the strong interaction regime is approached. Thus, using the strong interaction expansion, we find

$$\frac{L}{\delta} \sim \bar{\chi}^{\frac{\gamma+2}{2\gamma}-\frac{3}{2}}$$

or approximately,

$$\frac{L}{\delta} \sim \frac{1}{\sqrt{\bar{\chi}}}$$

It is concluded then, that the L/δ ratio goes to a constant as the Blasius point is approached and tends to zero as the leading edge is approached. These qualitative results have particular significance in regard to the pro-

per numerical procedures for boundary layer analysis. In particular, if the departure solutions are to be "suppressed", the integration must be done implicitly with a step size larger than L. If the departure solutions are desired, then the step size must be much smaller than L. Before leaving this point, it should be mentioned that the implicit numerical integration procedure used in this study will give, at each step of the calculation, the three eigenvalues associated with the linearized problem. If the point in question is on the relaxation surface then one eigenvalue is generally much smaller than the other two and corresponds to the above departure lengths. It may well be that for certain problems a preliminary survey via the moment method of the L/δ ratio would be of help in attempts at numerical integration of the full partial differential equations.

3.3.3. The "Departure" Integrals And "Upstream Influence"

The "departure" solutions form a two-parameter family - the parameters locating the departure point on the relaxation surface. Or more precisely, since the departure is exponential, one can assign one parameter to tag the integral curves in the surface and the other to measure

the extent of departure from any arbitrarily chosen point on the surface. If one considers only those solutions departing from the surface integral which passes through the leading edge singularity, then the departure solutions are characterized by only a single parameter. It is this latter family that is usually referred to as the "free interaction" solutions - although the entire two-parameter family will be implied herein by "free interaction" unless specifically referred to as "leading edge free interaction". The name "free interaction" is chosen to convey the idea that the boundary layer can respond to a downstream disturbance without the need for stimulus from the wall or from an incident wave impinging from the outside. Physically, of course, this reflects the fact that the downstream disturbance can propagate upstream through the subsonic portion of the layer. The lack of departure solutions on the supercritical side is a consequence of an effective cut off of the subsonic channel.

All solutions corresponding to the upstream influence of any arbitrary disturbance on a flat plate must fall in this two-parameter class. The eventual return to Blasius is accomplished through a mechanism not described by the flat plate equations with a waves-of-one-family (Prandtl-

Meyer) interaction equation. The only way the moment method equations can yield a smooth return to Blasius after "departure" has taken place, is for one or both of the above constraints to be dropped, i.e. either wall curvature or incident waves at the outer edge must come into play.

To conclude this section some estimates for the length of upstream influence are given. For the expansive "free interactions" the "departure length" L is probably a fairly close estimate for upstream influence for all expansive disturbances. It is likely that nonlinear effects on the perturbation occur over only a short distance of the order of a boundary layer height in the immediate neighborhood of the disturbance. Hence a linear theory such as Lighthill's should adequately give the upstream behavior up to a point very close to the disturbance. Further, one anticipates that the linear departure solution given earlier (equation 3.3) should agree with Lighthill's result. For comparison purposes we take $\rho\mu$ = constant and $\mu \propto T$, then Lighthill's result is

$$\frac{L}{x} = 4.78 \left(\frac{\gamma-1}{2}\right)^{\frac{3}{2}} \bar{\chi}^{\frac{3}{4}}$$

and comparing, we have for small $\bar{\chi}$

$$L_{\frac{\text{Linear-Prandtl equations}}{\text{Linear-moment method}}} = 0.63 \left(\frac{\gamma-1}{2}\right)^{-\frac{1}{2}} \bar{\chi}^{-\frac{1}{4}}$$

which for $\bar{\chi} = 0.5$ equals 1.67.

Hence, good agreement exists between the two results considering the roughness of the estimate.

For compressive disturbances the linear theory will fail to predict the upstream influence length since here the nonlinear aspects persist over many boundary layer heights upstream of the disturbance. The length of the upstream influence will, unlike the expansive case, depend on the nature and strength of the disturbance. Lewis (8) has reviewed the estimates of this length made by Chapman, Curle and Lees. He finds general agreement between the three estimates, which indicate that if the disturbance strength (fractional pressure rise) is scaled by $\sqrt{\bar{\chi}}$, then L/x also is proportional to $\sqrt{\bar{\chi}}$.

3.4. A Review Of The Fundamental Assumptions Of The Moment Method

Some questions which reflect the fundamental assumptions can be put as:

1) Is the one-parameter family of profiles chosen to represent the flow adequate?

2) Is the choice of governing equations adequate?

3) Is the omission of a lateral pressure gradient reasonable?

4) Is the boundary layer edge definition adequate?

In each case it is hard to assess the effect of the assumptions, especially those reflected by 1) and 2) above. The ultimate justification, of course, lies with the method's ability to satisfactorily predict experimentally verified behavior. The correlation with experiment of the expansive corner solution contained in this study is not completely satisfactory on the downstream side of the corner. The trouble may rest with any one of the implied assumptions. For example, in the expansion process the stream tubes in the outer portion of the layer are, relative to the inner stream tubes, accelerated very little in the neighborhood of the corner. The consequence is a "sinking" of the profile with an attendant large increase in wall shear but small change in the outer nature. The Falkner-Skan family does not contain such profiles. Furthermore, in order to achieve the high wall shear with the Falkner-Skan family, the physical location of the "edge" has a tendency to come nearer the wall. If the edge comes in too close it amounts to allowing fluid to leave the boundary layer. Such fluid is vortical and hence the

the Prandtl-Meyer interaction equation may be inadequate. The whole question of edge definition is linked to the absence of and relative importance of the lateral pressure gradient at the edge. If the lateral pressure gradient is retained, the location of the edge is immaterial provided the outer flow is truly inviscid.

The choice of governing equations may be the most subtle of all. If the profile family were absolutely complete in the sense of containing all the exact solution profiles for the problem at hand, then any independant set of governing equations compatible with the full boundary layer equations would be satisfactory. The profile family is not complete, of course, but hopefully the deviation occurs only in small, relatively unimportant details of the profiles. The general rule for selecting the constraining equations then, is that they must not be too restrictive with respect to the behavior of "small details" of the profiles. An excellent example is pointed out by Lees and Reeves (1) in regard to separation flows. If the boundary layer differential equation is invoked at the wall, it insists on a very special detail behavior, namely that

$$\frac{\partial^2 u}{\partial y^2} = 0 \quad \text{if} \quad \frac{\partial P}{\partial x} = 0 .$$

Hence it eliminates the possibility of being able to generate with the Falkner-Skan family a reverse flow profile in the pressure plateau region of separation. The Falkner-Skan family cannot satisfy that detailed requirement.

One anticipates that the inclusion of the lateral pressure gradient is probably crucial in situations of very rapid expansion such as sharp corner flow.

As discussed in Section 2, a highly expanded full boundary layer with a large mean Mach number responds to a downstream disturbance with a very short length scale and with a significant lateral pressure gradient. The moment equations cannot predict such a response of a supercritical layer because of the absence of the lateral pressure gradient. The suggested procedure (1) in such situations is to allow a discontinuous "jump" to a subcritical state. The "jump" conditions are established by conserving mass and momentum between the jump stations, and by assuming the scale is sufficiently short that the flow responds isentropically. The latter is equivalent to the assumption that the dissipation terms in the energy equation can be ignored. The question remains open as to how satisfactory this approach is.

3.5. The Numerical Approach

The set of equations (3.1) were approximated by an implicit finite difference set of equations which in turn were programmed for solution on an IBM 7094 electronic computer. The implicit method consists of locally linearizing the RHS of the equations at each step. The difference formulation of the resulting linear set is such that the RHS is evaluated at the next, as yet unknown, step. The derivatives on the LHS were represented by the usual simple-Euler difference, or as an option for greater accuracy, a back point was incorporated in this difference representation. The resulting set of three coupled algebraic equations is then solved for the new solution vector at the forward step. The great drawback to such an approach is that it is tedious to program. Explicit integration such as Adams-Moulton is, of course, much faster. However, typical problems involve only a fraction of a minute with either method so this is not an issue.

The motivation for implicit integration was to be able to integrate the equations starting near the leading edge singularity much as had already been done implicitly by Flügge-Lotz and Blottner (9) and Mann and Bradley (10) with the full boundary layer equations.

Systems which possess an exceptional integral path, from which neighboring solutions diverge rapidly, are difficult to handle numerically if one wants to pursue the exceptional path. Such a situation is usually considered as poorly posed as an initial value problem. If one knows or can establish the downstream boundary conditions, it is often desirable to treat the problem as a boundary value problem. However, if circumstances compel one to treat it as an initial value problem, implicit methods offer a powerful technique. This was first pointed out by Curtiss and Hirschfelder (11) who were motivated by problems in the chemical kinetics of detonation. In effect, if one takes step sizes larger than the "departure" scale, the "departure" solutions are suppressed. And since the characteristic length associated with the exceptional path is large, the truncation error will generally be small. If it is desired at some station to pursue a departure path it is only necessary to decrease the step size until it is well below the "departure" scale.

As it turns out, however, the moment equations still will not yield to numerical integration out of the leading edge. The approach was to get somewhat removed from the leading edge by means of the leading edge expansion and

then procede via an implicit method. The RHS of equations (3.1) are so strongly nonlinear near the leading edge that when a step size large enough to suppress the departure solutions is attempted, the resulting nonlinear algebraic set of equations appears to be impossible to solve. All manner of attempts at finding a "predictor" to establish a good first guess for this solution failed. The Newton-Raphson iteration procedure simply would not converge under any amount of prodding.

Although it was known that the leading edge had a strong saddle as well as node character, it was decided to try and brute force one's way into the leading edge by starting downstream and integrating backwards. The question then was what represented a legitimate family of initial conditions which could be used in an iteration procedure to locate the leading edge. It was in the process of numerically experimenting with various initial conditions that it became apparent that, regardless of the initial choice, the paths relaxed to a single surface upon backward integration. The surface was then developed in some detail and the integral path approaching the leading edge was established. In establishing the leading edge integral it was found that the saddle-like behavior was

entirely too severe to be able to penetrate into the leading edge by iterating on the initial location in the surface far downstream. However, with the surface now partially defined, it was possible to push towards the leading edge until the path started to diverge and then iterate in that neighborhood on the surface for new initial data which would allow a still closer approach to the leading edge. After several cycles of such a procedure the desired solution was obtained.

Hence the implicit feature of the integration procedure was never really utilized. It has been mentioned here primarily as background for the implicit integration employed with the full partial differential equations in Section 4.

The surface thus generated by backward integration was found to contain the "critical line". Backward integration could not be pushed, even implicitly, beyond the critical line. Apparently, again, the nonlinearity of the RHS of equations (3.1) is too severe.

Again by experimentation it was found that forward integration on the supercritical side from essentially arbitrary initial points produced a rapid <u>decay</u> to a well defined surface and from there the integrals eventually

passed into the critical line. The paths which meet from both sides at the critical line are continuous, well behaved, and clearly represent the same integral.

Verification that the subcritical relaxation surface, as generated, is truly what is being claimed, was made by integrating forward from various randomly chosen points on the surface. The result, as expected, was rapid divergence from the surface on one side or the other. If one allows a small departure of this sort and then "reflects" the perturbation about the departure point and takes that condition as the initial value then the departure is to the opposite side.

Finally, as an example of continuous expansion from supercritical to subcritical, the flow around a relatively sharp corner was analyzed. No specific physical problem was studied but rather the calculation was performed in a way that minimized the computational effort.

3.6. The Results

3.6.1. The "Relaxation" Surface

Figures 3,4 and 5 describe the subcritical surface generated by using the Prandtl-Meyer interaction equation. This surface does not contain the leading edge

singularity because of the use of the Prandtl-Meyer interaction equation. The question, then, is which of the integral curves would pass through the leading edge singularity if it was continued at some appropriate matching point by a solution generated using the tangent-wedge interaction equation. Such an integral curve was established by 1), assuming the tangent-wedge extension would be a straight line in the $Re_{\delta_i}^*$ -a plane, and 2), by taking the leading edge value of a=2.29, which results from the strong interaction expansion.

Figures 6 and 7 describe the surface as generated using the tangent-wedge interaction equation. The solutions here include a portion of the supercritical surface. The surface contains the leading edge solution which was extended below $Re_{\delta_i}^* = 125$ by extrapolation.

3.6.2. The Infinite Flat Plate Solution

Figures 8 and 9 give the infinite flat plate solutions with Prandtl-Meyer and tangent-wedge interaction equations respectively. $Re_{\delta_i}^*$, M and "a" are given as a function of $\bar{\chi}$. Comparison is made with the "weak interaction" expansion in Figure 8 and the "strong interaction" expansion in Figure 9.

P/P_∞ vs. $\bar{\chi}$ is given in Figure 10 and compared to the data of Reference (12). The agreement is good.

3.6.3. Expansion Corner Solution

The corner results are presented in Figures 11,12 and 13. The hypersonic pressure-Mach number relation was used which may be the source of some error. It has been found by K. Victoria (13) that experimental data in this general M, $Re_{\delta_i}^*$ and angle range can be collapsed into a single curve of

$$\frac{P-P_{\infty+}}{P_{WIL}-P_{\infty+}} \quad \text{vs.} \quad (x-x_c)/\delta \quad \text{For} \quad \frac{x-x_c}{\delta} < 0$$

and

$$\frac{P-P_{\infty+}}{P_{WIC}-P_{\infty+}} \quad \text{vs.} \quad (x-x_c)/\delta \quad \text{For} \quad \frac{x-x_c}{\delta} > 0$$

where P_{WIL} is the local value of the weak interaction pressure in the absence of a disturbance; P_{WIC} is the weak interaction value at the corner location; and x_c locates the center of the corner. The result is apparently independent of the corner radius provided the length of the curved portion is not greater, say, than a few boundary layer heights.

4. FINITE DIFFERENCE SOLUTIONS OF THE "GENERALIZED" LAMINAR BOUNDARY LAYER EQUATIONS

4.1. General Discussion

Can the class of local interaction problems under consideration in this study be treated by the numerical integration of a suitably generalized form of partial differential field equations governing thin viscous layers? The portion of the investigation presented in this Section is directed toward resolving this question.

Before examining the numerical procedure and results, let us begin by anticipating where difficulties might lie in this approach. First of all, we expect the same qualitative behavior as that exhibited by the moment method solutions; that is, there exists a "relaxation" solution tending to Blasius on a flat wall with solutions departing from it on a relatively short scale length. We expect this departure length, relative to the boundary layer height, to increase from a very small value near the leading edge to something like a couple of boundary layer heights as we proceed to low $\bar{\chi}$ values.

In regard to the nature of the "departure" solutions, our chances for success rest on several key points. First of all, we hope that we can generate a physically meaning-

ful one-parameter family of free interaction solutions. If the departure solutions are critically dependant on the fine detail of the functions describing the boundary layer, then the problem is indeed "poorly posed" and must be treated as a boundary value problem. The latter approach would appear to be exceedingly difficult. But such a procedure is not necessarily out of the question, especially in the light of recent successes in numerical experimentations of very low Reynolds number flows and supersonic inviscid flows with imbedded subsonic regions. The approach here, however, is to proceed by the far easier forward marching technique in the hope that it will be successful for at least an interesting class of problems.

Now of course the equations must possess an infinite variety of departure solutions, differing in very fine detail initially but eventually becoming a clearly discernible multi-parameter family of solutions. If one thinks of the departure as a linear phenomena, analogous to the Libby and Fox (5) treatment of non-interacting flows, then the departure can be envisioned as a superposition of eigen solutions. The success of the numerical forward marching approach will rest on the correctness of the assumption that the scales associated with these departure modes are

well displaced. Hence the "fine" structure associated with an initial perturbation will decay quickly leaving a single "fundamental" mode. It is clear that the very essence of this approach precludes the analyzing of problems in which very fine detail is desired. For example, suppose one wanted to know the detailed flow around a small probe imbedded within a separated region. Obviously there is no chance that one could treat such a situation by an initial value technique. The manifestation of the presence of the probe on the character of the flow well upstream is infinitesimal, yet that is where one would be attempting to describe the solution initially. On the other hand, if we are willing to accept less detail, we might hope for a reasonable solution removed slightly from the probe.

The question then is, if we are successfull in generating a "smooth" one-parameter family of departure solutions, can these be used to represent the upstream influence for a physically interesting class of problems. We anticipate that we will be restricted to a class of problems with a certain degree of "smoothness" and that in the neighborhood of regions which lack this, we must be willing to accept loss of detail. This situation is not a new one, a now classic example being Van Dyke's treatment of the

inviscid flow over blunt bodies at supersonic flight speeds. In that case he treats the subsonic region behind the shock as an initial value problem. A smooth conic section shock shape is selected and produces a "smooth" body shape.

So far what we have anticipated in the way of mathematical behavior stems, in large part, from a knowledge of the moment method solution. To recap, we have implied that "relaxation" solutions exist and that success in this approach will lie in being able 1) to generate such a solution; 2) to suppress or trigger departure from it at any desired position; 3) upon departure, to suppress all fine structure disturbances and retain only some dominant solutions; and finally, 4) to show that such a solution is not just a solution to the difference equations for which we have suppressed all the "real" solutions, but that it is indeed a solution to the differential equations.

The issue of whether one can properly pose a problem as an initial value problem, is fundamentally linked to the sensitivity of the subsequent solution to the initial data. This in turn can be associated with positive exponential solutions in linear systems. Elliptic equations are the prime example of poorly posed initial value problems. This

can be thought of as a consequence of the existence of positive exponential solutions off of the initial surface. The heat equation integrated in negative time is another example. Thus we can discern at least three aspects which may give trouble and a knowledge of these will be helpful in attempting to surmount the problems. First, as we have mentioned, there is a positive exponential nature associated with the interaction equation. Secondly, the boundary layer equations are diffusive in nature when the viscous terms are comparable to the inertia terms - hence in regions of reverse flow, analogous to integrating in negative time, we can expect trouble. And thirdly, if the lateral pressure gradient is retained, then under circumstances where perturbations of small scale length exist, the subsonic region will behave inviscidly and hence elliptically, thus exhibiting positive exponential solutions.

As if the above wasn't bad enough, we must now interject an additional and important consideration. The above discussion reflected the character of the differential equations. The question now is, do the difference equations introduce additional spurious positive exponential or oscillating behavior, i.e. numerical instability?

4.2. The Differential Equations

In order to avoid the complete ellipticity of the Navier-Stokes equations, the Stokes-like viscous terms associated with $\frac{\partial^2}{\partial x^2}$ were dropped where x corresponds to the coordinate aligned with the flow. Inclusion of such terms would preclude the treatment as an initial value problem.

The Navier-Stokes equations are reduced by one order under the fundamental assumption that viscous regions will be confined to thin layers aligned with one of the coordinate directions. Other than the dropping of the Stokes-like viscous terms which involve $\frac{\partial^2 u}{\partial x^2}$ and $\frac{\partial^2 v}{\partial x^2}$, the full equations have been retained pretty much intact. The terms dropped are so called Stokes-like because, if the viscous region is truly thin, then simple order of magnitude estimates indicate that these quantities can be of significance only in regions where the inertia terms are tending to zero. In addition, a very short characteristic length disturbance, such as that introduced for example at a sharp corner, is required in order for these terms to be significant. The extent of such a region is of the order of the "Stokes radius" or the radius at which the local Reynolds number is unity. The "Stokes radius" to boundary

layer thickness ratio is about 1/20th at a plate Reynolds number of 100,000.

The major difference then between the set of equations dealt with here and the usual Prandtl boundary layer equations, is the inclusion here of the lateral momentum equation with its attendant lateral pressure gradient. Of secondary interest, for the present, was the inclusion of lateral viscous and dissipation terms in order to properly describe imbedded shocks aligned with the x-axis. The inclusion of the latter might also allow solution of the combined shock structure-boundary layer problem at the leading edge.

The equations were written in axisymmetric orthogonal surface coordinates and derived under the single assumption that the viscous layer, whether shock or shear like, is thin and aligned with the surface coordinate. All transverse and longitudinal curvature terms are retained so the system reduces to the correct polar coordinate formulation at a sharp corner and reduces properly for the axisymmetric wake case.

After writing the equation in curvilinear coordinates and making the "thin viscous layer" assumptions, the coordinate transformation $(x,y) \rightarrow x, \eta = F\ (y/x^n)$ was intro-

duced to facilitate the numerical treatment. F is an arbitrary analytical function. The transformation allows one to conveniently vary the mesh spacing in the lateral direction depending on the problem at hand. Simplifications using Crocco or stream function coordinates are not possible since reverse flows are to be considered. No advantage or simplification was felt to be gained by the introduction of a Howarth transformation.

Since the equations contain the full inviscid equations they could, in principle, be integrated out to a point sufficiently far removed that the disturbance vanished, and that could serve as the complete formulation of the problem. In practice, that generally requires far too many node points if one retains the implicit numerical formulation required within the viscous portion. The leading edge might be an interesting exception. The alternative is to change the method of calculating the flow field outside of the vortical region of the viscous boundary layer. The most general approach is to use the method of characteristics or simply an explicit forward marching along coordinate lines. If the latter is used, care must be taken to insure that the "region of influence" of a field point falls entirely downstream of the coordinate line.

Mann and Bradley (10) employ rotational characteristics in their study of the leading edge interaction problem. The approach taken here is to adopt a simple model for the outer flow; either tangent-wedge theory or the simple wave flow described by the Prandtl-Meyer relation. Hence the study has been restricted to those situations for which no disturbance is imposed on the flow from outside the boundary layer. What has been investigated are the "free interactions" which can represent the upstream influence associated with disturbances imposed from outside the layer, and corner flows where the disturbance originates on the wall side of the layer.

The Navier-Stokes equations in orthogonal curvilinear coordinates are given, for example, by Tsien (14). The equations used here in reduced form are in Appendix 3.

Boundary conditions at a solid wall were prescribed with the allowance for arbitrary blowing and wall temperature distribution. Thermal fluid properties were allowed to have arbitrary temperature dependance.

4.3. The Difference Equations

The differential equations as given in Appendix 3 were approximated by linear difference equations utilizing a fully implicit differencing scheme as distinguished from

the Crank-Nicholson averaging method. That is, the x derivatives are all evaluated at the downstream node point - not an intermediate point. To gain second order accuracy, the use of a back point in the difference representation of $\frac{\partial}{\partial x}$ was provided as an option. In order for the implicit difference equations to be linear, the dependent variables themselves (as distinguished from their derivatives) were evaluated at the upstream node points for the first evaluation of the solution at the downstream node. Iteration at the downstream node was provided for to reduce the error associated with this linearization. The difference relations used are in Appendix 4. Motivations for the above choice are as follows. First, an implicit method is necessary for diffusion equations regardless of any additional complications if reasonable step sizes in x are to be tolerable. In addition, we want to make use of the fact that a fully implicit method will be the most effective in suppressing the anticipated "departure" solutions. Again, the reader is referred to Reference (11) for discussion of this point. That such suppression can be achieved even with the Crank-Nicholson implicit formulation has already been demonstrated by the very fact that Flügge-Lotz and Blottner (9) obtained well behaved, bounded solutions in treating

the large $\bar{\chi}$ leading edge interaction problem. In general the choice here was made on the basis of obtaining the most stable method possible. Comparable accuracy to the Crank-Nicholson method is obtained, as mentioned, by the use of an additional back point and by iteration. It should be noted that the Crank-Nicholson approach also needs to incorporate an iteration to achieve second order accuracy.

In anticipation of difficulties in the subsonic region, an option was programmed whereby, below any prescribed value of η or Mach number in the flow, the lateral momentum equation is replaced by the condition that the lateral pressure gradient is zero.

The edge definition was taken as that value of η for which the velocity and temperature gradients fell below specified values. If the number of nodes is insufficient to be able to realize this condition, the mesh is extended outward. The linear system of difference equations form a banded matrix of dimension 4N by 15 where N is the number of lateral mesh points. These are solved using a band matrix inversion routine which is very efficient.

4.4. The Results

All calculations were carried out for $M = 5.8$; $\mu \sim T$; and $Pr = 1.0$. Except near the leading edge, where the tan-

gent-wedge approximation was used, Prandtl-Meyer outer flow was assumed in all cases. All examples were for an adiabatic, impervious wall.

4.4.1. Infinite Flat Plate

The infinite flat plate solution was obtained starting at the leading edge and progressing downstream to the weak interaction regime. Departure solutions are effectively suppressed by taking steps which become increasingly longer relative to δ as the integration proceeds downstream. The step size becomes approximately 2δ as the weak interaction region is reached. The numerical accuracy is good near the leading edge where $\Delta x/\delta$ is small. The accuracy is also good in the weak interaction region where, although $\Delta x/\delta$ is approximately 2, the boundary layer is changing slowly. These conclusions are confirmed by increasing the step size in these regions without an appreciable change in the results. In an intermediate region between these extremes, where $\bar{\chi}$ is between 2.0 and 4.5, the accuracy is not so good. The required step size of approximately one boundary layer height apparently gives rise to too large a truncation error in this region where the relaxation solution itself is still undergoing rapid change. In this range of $\bar{\chi}$, the generated pressure dis-

tribution was taken as prescribed input in a non-interacting boundary layer calculation using the interaction solution at $\bar{\chi} = 4.5$ for initial data. The integration was performed on a very small step size to insure accuracy. The resulting lateral velocity at the edge, when compared with the interaction calculation, showed approximately a 5% to 10% disagreement. No attempt was made to improve this solution, although iteration on the pressure field would undoubtedly yield an accurate solution. It is also quite likely that further experimentation with regard to an optimum step size distribution might help.

The primary goal of obtaining an accurate, self consistent solution in the $\bar{\chi} < 2$ range was achieved. This was then used to investigate the "free interaction" departures.

Initial profiles for the leading edge problem were obtained from the leading edge similitude solutions (15). These are given in Figures 14 and 15.

Figure 16 gives the pressure distribution in the immediate vicinity of the leading edge. This calculation was performed with step sizes of both one-half and one boundary layer height with no significant difference in the result. Results were obtained both with and without

iteration to reduce the linearization error associated with the difference equations. This was found to be a significant factor. Further, it was found that a single iteration was satisfactory and this was done in all subsequent problems. Figure 16 shows the effect of cutting the step size back to 0.1δ and 0.03δ - immediate departure results. Figure 17 shows the pressure distribution for the entire $\bar{\chi}$ range and compares it with experimental data and the weak and strong interaction expansions.

Finally, it is noted that even though the numerical accuracy appears good for $\bar{\chi} > 5$, the agreement with experimental observation is not so good. For the leading edge calculations of this section the lateral pressure gradient was set equal to zero. This, in conjunction with the use of the tangent-wedge interaction equation, probably invalidates the results for $\bar{\chi} > 5$ where $Re < 1500$ and the usual boundary layer assumptions become questionable. The edge definition in particular becomes an important factor in regions of rapid expansion if the lateral pressure gradient is not properly accounted for. This point has not been investigated further as of this writing. In all subsequent calculations the lateral pressure gradient has been included at least in the supersonic portion and hence the

edge definition is not an issue.

4.4.2. The Free Interaction Solutions

The equations do exhibit a one-parameter family of "free interaction" solutions departing from the infinite plate solution. (Henceforth, the semi-infinite flat plate relaxation solution, exhibiting the leading edge singularity, will be referred to simply as the "infinite plate" solution. Any other relaxation solution on an infinite plate, such as the "reattachment" solution in which a separated flow returns to the wall and passes downstream to the Blasius point, will be specifically defined.) These free interaction solutions can be generated by cutting back the step size in x from the large value used to suppress them. Examining the behavior as the step size is reduced, one finds the following. For only a small reduction, the same "relaxation" solution is recovered. When Δx is substantially cut back, say from 2δ to δ, then an erratic oscillatory behavior sets in. The solution apparently tries to drive off on a departure solution and is returned by the implicit "restoring" mechanism. Then, upon further substantial reduction, smooth well behaved departure solutions are generated. It is found that once on a departure

integral, there is a clear and easily established step size below which the integration is accurate, i.e. further reduction in step size does not alter the result. The "rate" of departure can be increased by "kicking" the solution substantially off the relaxation solution in the first departure step. That is, it is possible to jump onto an integral curve which departed from the relaxation solution considerably further upstream. It is found that some caution must be exercised if one attempts the latter. An arbitrary "kick" or perturbation of the relaxation solution does not yield a solution which belongs to the "infinite plate" one-parameter family. This is precisely the same situation as was found with the moment method. However, for $\bar{\chi} < 2$, it appears that regardless of the nature of the initial perturbation, the solution within a few boundary layer heights at most does settle into the one-parameter family associated with the "infinite plate". Hence the only uncertainity in using such "arbitrary" departure conditions is in the initial behavior, not downstream in the neighborhood of the disturbance giving rise to departure. One convenient method of "kicking" is to take an intermediate sized initial step - not so large as to remain on the relaxation solution and not so small as to give a

gradual departure. In other words, this is just a simple way of getting the computer to make a small initial "mistake". The initial step size can be used as a parameter to generate the entire family. Within a short distance the family so generated takes on the characteristics of the one-parameter "infinite plate" family.

Figure 18 shows members of the family as generated from two different departure points using various initial step sizes. Solution D gives an example of too large an initial kick - it takes some distance before the solution settles into its ultimate role as a member of the family. Initial conditions for solution C were generated in a different manner. An already generated expansive departure was selected and its deviation from the relaxation solution was calculated in terms of a perturbation distribution in η of U, V, P and T. The sign of these perturbations was then changed and the initial conditions for solution C were thus established. The resultant solution soon falls into place as an acceptable member.

Figures 19 through 24 give the detailed character of a representative expansive and compressive free interaction solution. The transverse momentum equation is retained throughout the layer in the expansive case. No subsonic

instabilities developed until the flow was expanded around a sharp corner. Downstream of the corner it was found necessary to restrict the transverse momentum equation to the supersonic portion and to assume zero pressure gradient normal to the wall in the subsonic region. In the compressive case the gradient was retained to the wall until the proximity of the separation point was reached. Following that, instabilities dictated that the non-zero transverse gradient of pressure be restricted to the supersonic regime.

4.4.2.1. Separation And Reverse Flow

Perhaps the most interesting result of all is the compressive free interaction solution passing smoothly through separation and well downstream into the reverse flow field. The so called "pressure plateau" or leveling off of the pressure rise is clearly discernible in Figure 22. Figure 23 presents the velocity profiles at various stations beginning with a near-Blasius weak interaction profile and ending with a profile which is approaching the free mixing solution.

Figure 23 shows, however, a severe shortcoming of the solutions obtained to date. There is an oscillation at the edge in all the boundary layer variables which first devel-

ops either at or slightly prior to separation. This undoubtedly has effected the interaction considerably. Figure 25 shows the corresponding pressure oscillations. Comparison with the experimental results of J. Lewis (8) indicate that the x-scale length obtained here is too long by about 30%. Until the edge oscillation is rectified it does not seem worthwhile to conjecture further on this discrepancy. It is known that the Falkner-Skan similitude equation for negative β's does not have a unique solution. The proper solution is chosen on the basis of correct matching to the outer flow. This requires that the deviation of the boundary layer solution from the outer solution must be transcendentally small as the boundary layer variable tends to infinity. It may be that the numerical solution obtained here corresponds to one of the inadmissible Falkner-Skan solutions and must be eliminated on the basis of improper matching. On the other hand, the Libby-Fox (5) non-similar near-Blasius solutions for relaxing flows show oscillatory behavior which exponentially decays at the edge. Hence, because the solutions are oscillatory is probably not sufficient reason to artificially suppress them. It is probable that these oscillations are the result of numerical instability linked to the reverse flow

region; although no perceptible signs of instability are seen in the reverse flow region until well downstream of the initiation of the outer oscillations. In the absence of a turn in the wall, the reverse flow develops a numerical instability about three boundary layer heights downstream of separation. This instability appears primarily in the V velocity component, and oscillations (except at the edge) do not appear above the dividing stream line. It is interesting to note that for a smooth compressive turn, the reverse flow is apparently stabilized, at least as far downstream as the calculation was carried in this study. In addition, the presence of a smooth turn causes the outer oscillations to damp out and eventually disappear. The velocity profiles associated with such a turn are given in Figure 32. These can be compared to those in Figure 23. Separation is at the same location in both cases.

In Figure 24 a typical reverse flow profile is shown as a function of the Howarth coordinate and is compared to the similitude reverse flow solutions found by Stewartson. These solutions were computed by Klineberg (3). The comparison shows a close family resemblance.

4.4.2.2. Expansion And The Critical Point

Figure 18 shows the precipitous manner in which the pressure falls for expansive free interactions. As a consequence, a numerical solution for the final stage of this plunge is difficult to achieve.

There is a limiting case, for expansive upstream influence, in which the sonic line comes into the wall. Such a singularity is possible for the equations we are dealing with because of the absence of the Stokes-like region. The picture quite probably is the following. The flow perturbations respond in an inviscid manner in regions where the streamwise gradients become large. The thin viscous sublayer adjacent to the wall is of the backward boundary layer type with flow emerging from it into the inviscid domain. In the limit mentioned the streamwise gradients near the wall become very large and the viscous wall layer vanishes. Such a solution cannot be continued downstream unless a sharp corner is present with an angle greater than some "critical" value. The "critical" angle is of such a magnitude that all the stream tubes can swell in accordance with the falling pressure, while the outer stream line inclination becomes progressively more negative in accordance with the outer simple-wave flow. This singularity is the

direct analogue of the moment method critical point. The entire layer is supersonic and it cannot respond further to changes in downstream conditions.

4.4.3. Expansion Corner

Figures 26 through 30 present the results for flow over an expansion corner of approximately 7.4 degrees. The upstream Mach number is 5.8 and the corner Reynolds number is 123,000. The corner radius of curvature is $0.9\ \delta_c$, where δ_c is the boundary layer height at the corner. The upstream-influence portion of the solution corresponds to curve D of Figure 18.

The solution procedure was to vary the corner angle until, in effect, the downstream boundary condition was met, keeping the upstream solution fixed. As the angle is varied, the solutions either go to a compressive separation-type behavior or to an expansive "critical point" type behavior. It is the exceptional integral which neither goes to separation nor the "critical" point that will satisfy the downstream boundary conditions that the flow be attached and approaching the pressure level corresponding to the Prandtl-Meyer turn. This was the easiest procedure to adopt for demonstrative purposes. Figure 25 shows the

nature of the integral curves as the angle is varied. The angle was varied in 0.1 degree increments which were satisfactory to establish the solution for about three boundary layer heights downstream. The calculation was not continued beyond that point. The data compilation of K. Victoria (13) is given in Figure 25. The agreement downstream is good, although possibly fortuitous in light of the differences in the defining parameters between the experimental and computed cases. A one-quarter boundary layer height origin shift would bring the upstream data into essentially exact agreement. Figure 27 gives the downstream pressure profiles. $\frac{\partial P}{\partial y}$ and $\frac{\partial P}{\partial x}$ at the edge are consistant with simple wave flow. Beginning at the first downstream station the lateral pressure gradient below the sonic line was set equal to zero. A discontinuity in gradient thus appears at the first station of Figure 27. Figure 28 gives the downstream U-velocity profile as a function of the stream function.

Figure 29 presents the streamline pattern for the expansive corner. In addition, the Mach lines and a downstream constant pressure line are given. The downstream constant pressure line shown lies very close to a Mach line. The indication is that for small corner angles and within

a boundary layer height or two from the corner, wave reflection off of the shear layer is weak.

4.4.4. Compression Turn

A compression turn starting at a plate Reynolds number of 202,000 was briefly investigated. The radius of curvature was approximately 37 boundary layer heights. In terms of the plate length, the radius of curvature equals $2.9x_c$, where x_c is the location of the beginning of the turn. The calculation was terminated, after the flow had been turned approximately 5 degrees, due to numerical instability. No attempt has been made at this time to rectify the situation. Figure 30 gives the pressure distribution for this case. It qualitatively has very much the same behavior as that reported by Lewis (8) in his experimental investigation. The outer edge oscillations which exist between the separation point and the corner are damped out by the presence of the turn. Figure 32 gives the velocity profiles.

Figure 31 shows the streamline pattern for the separated region.

5. CONCLUSIONS

5.1. Moment Method Analysis

The most sweeping conclusion to be drawn is that the moment method equations offer a remarkably clear "picture" of supersonic laminar boundary layer mechanics. This in itself, completely aside from considerations of the detailed predictions, makes the moment method a valuable analytical tool.

5.1.1. The Blasius Point

The Blasius point is characterized by a one-parameter family of solutions relaxing into it. This family generates a "relaxation" surface in the phase space M, a, $Re_{\delta_i}^*$, which includes the leading edge and the critical line singularities. The asymptotic nature of the solutions going into the Blasius point are described by the infinite flat plate "weak interaction" expansion. The particular integral in the surface which passes through the leading edge singularity corresponds to the semi-infinite flat plate.

5.1.2. The Leading Edge

The leading edge is an isolated node-saddle singularity. The exceptional node path corresponding to

the flat plate solution is described by the "strong interaction" coordinate expansion.

5.1.3. The "Critical" Line

The "critical" line singularity has a nodal character. Integrating in positive x the paths converge toward the relaxation surface on the supercritical side, pass through the singularity and diverge on the subcritical side.

5.1.4. The "Departure" Solutions

On the subcritical side, all integral paths not on the surface diverge from it with increasing x. These represent the "free interaction" expansion and compression solutions.

5.1.5. The Expansion Corner

It was found possible to generate expansion corner flow solutions passing smoothly from subcritical to supercritical flow at the corner and returning smoothly to subcritical flow downstream on the flat wall.

5.1.6. The Infinite Plate Solution

The infinite plate solution was extracted from the relaxation surface and presented as a function of $\bar{\chi}$.

Agreement with experiment was found to be good.

5.2. Finite Difference Solutions Of The "Generalized" Boundary Layer Equations

The underlying conclusion of importance here is that a large class of physically interesting problems exists which can be successfully posed as initial value problems using these finite difference equations.

5.2.1. "Free Interaction" Solutions

The "free interaction" or "upstream influence" solutions departing from the infinite plate solution represent a one-parameter family. Their generation was found to be an easy matter of cutting back substantially on the step size required to generate the infinite plate solution. This again confirms the importance of implicit integration.

Separation solutions were obtained which penetrated into the reverse flow region for approximately three boundary layer heights before reverse flow instability sets in. These solutions, however, possess outer edge oscillatory behavior which has yet to be rectified. It seems likely that the problem is not insurmountable.

The expansion free interaction solutions support substantial lateral pressure gradients, indicating a definite

need for retention of these gradients.

5.2.2. Expansion Corner

Expansion corner flow for a 7.4 degree turn at M = 5.8 was obtained. The corner radius was approximately one boundary layer height. The solution was carried downstream for approximately three boundary layer heights. Agreement with experiment is good.

Continuation of the solution further downstream should offer no insurmountable problems.

5.2.3. Compression Turn

Preliminary investigation of a compression turn indicates a stabilizing effect on the reverse flow behavior. These preliminary findings lend some encouragement to the hope of carrying such a solution through reattachment. However, to do such would be asking a very great deal from an inverse technique. It may well be that once the flow is well separated, the best procedure would be to couple this numerical technique with the moment method.

5.2.4. General

Since the numerical approach offers considerable promise as an analytical tool for this type of inves-

tigation, additional exploratory work should be done. The range of applicability, the limitations, and the accuracy should be firmly established.

In particular, attention should be given to 1) the outer edge oscillatory behavior observed in this study, 2) the reverse flow instabilities and 3) inclusion of the transverse momentum equation near the leading edge.

5.3. Comparison Of The Two Approaches

It seems clear that the numerical integration of the full boundary layer equations is a powerful technique which should find an extensive role in analysis. It's potential for handling complex problems involving a multitude of "real" phenomena goes way beyond the moment method approach. The method should be adaptable to a wide variety of complexities including hard blowing, imbedded shocks, and chemical kinetics. Furthermore, by incorporating an appropriate orthogonal coordinate system, it seems likely that the near wake problem in the neighborhood of the body shoulder can be analyzed.

On the other hand, problems involving large scale separation certainly will require moment methods, or something equivalent to them, to handle the reverse flow por-

tion of the flow field.

The question of machine time requirements is often raised in a comparison of this sort. In general, however, once the procedures have been developed, the machine costs for complex problems of this sort are a small fraction of the total expenditure associated with the analysis effort.

REFERENCES

1. Lees, L. and Reeves, B.L.: "Supersonic Separated and Reattaching Laminar Flows: I. General Theory and Application to Adiabatic Boundary Layer/Shock Wave Interactions", AIAA J. 2:11 (Nov.1964).

2. Lighthill, M.J.: "Reflection At a Laminar Boundary Layer of a Weak Steady Disturbance to a Supersonic Stream, Neglecting Viscosity and Heat Conduction", Quarterly Jour. of Mechanics and Applied Mathematics, Vol. III, Part 3 (1950).

   Lighthill, M.J.: "On Boundary Layers and Upstream Influence: II Supersonic Flows Without Separation", Proc. Roy. Soc. (A). Vol. 217, p.478 (1953).

3. Klineberg, J.: Ph.D. Thesis, Calif. Inst. of Tech., Pasadena, Calif. (1967) To be published.

4. Lees, L.: "On The Boundary Layer Equations in Hypersonic Flow and Their Approximate Solutions", Journal of the Aeronautical Sciences, Vol. 20 No. 2 (1953).

5. Libby, P.A. and Fox, H.: "Some Perturbation Solutions in Laminar Boundary Layer Theory, Part I - The Momentum Equation", PIBAL Report No. 752 (1962).

6. Caughey, T.K.: Private Communication (1967).

7. Kubota, T.: Private Communication (1967).

8. Lewis, J.: "Experimental Investigation of Supersonic Laminar, Two-Dimensional Boundary Layer Separation in a Compression Corner With and Without Cooling", Ph.D. Thesis, Calif. Inst. of Tech., Pasadena, Calif. (1967).

9. Flügge-Lotz, J. and Blottner, F.G.: "Computation of the Compressible Laminar Boundary Layer Flow Including Displacement-Thickness Interaction Using Finite-Difference Methods", Stanford University Tech. Report No. 131 (1962).

REFERENCES (Cont'd)

10. Mann, W.M. and Bradley, R.G., Jr.,: "Hypersonic Viscid - Inviscid Interaction Solutions for Perfect Gas and Equilibrium Real Air Boundary Layer Flow", Journal of Astronautical Science, Vol. X, pp. 14 - 27 (Spring 1963).

11. Curtiss, C.F. and Hirschfelder, J.O.: "Integration of Stiff Equations", Proc. of the National Academy of Sciences, Vol. 38, No. 3 (1952).

12. Hayes, W.D. and Probstein, R.F.: "Hypersonic Flow Theory", Academic Press, New York, (1959).

13. Victoria, K.: Private Communication (1967).

14. Tsien, H.S.: Princeton Series on High Speed Aerodynamics. Vol. III: Fundamentals of Gas Dynamics Princeton University Press.

15. Li, T.Y. and Nagamatsu, H.Y.: "Similar Solutions of Compressible Boundary Layer Equations", GALCIT Memorandum No. 22 (Sept. 1954).

APPENDIX 1: DEFINING RELATIONS FOR MOMENT METHOD FORMULATION

A1.1. General

$$\delta_i^* = \int_o^{\delta_i} \left(1 - \frac{U}{U_e}\right) dY$$

$$\theta_i = \int_o^{\delta_i} \left(\frac{U}{U_e}\right)\left[1 - \left(\frac{U}{U_e}\right)\right] dY$$

$$\theta_i^* = \int_o^{\delta_i} \left(\frac{U}{U_e}\right)\left[1 - \left(\frac{U}{U_e}\right)^2\right] dY$$

$$\mathcal{H} = \frac{\theta_i}{\delta_i^*} \quad ; \quad J = \frac{\theta_i^*}{\delta_i^*}$$

$$R = 2\,\delta_i^*/U_e^2 \int_o^{\delta_i} \left(\frac{\partial U}{\partial Y}\right)^2 dY \quad ; \quad P = \frac{\delta_i^*}{U_e}\left(\frac{\partial U}{\partial Y}\right)_{Y=0}$$

$$Z = \frac{1}{\delta_i^*} \int_o^{\delta_i} \left(\frac{U}{U_e}\right) dY$$

$$a = \left[\frac{\partial\left(\frac{U}{U_e}\right)}{\partial\left(\frac{Y}{\delta_i}\right)}\right]_{Y=0}$$

$$Y = \int_o^y \frac{a_e \rho}{a_\infty \rho_\infty}\, dy$$

$$\delta = \int_o^{\delta_i} \frac{a_e \rho}{a_\infty \rho_\infty}\, dy = (\delta_i^*/\xi)\,[(1+m_\infty)/(1+m_e)]^{\frac{1}{2}}\,[1+m_e(\mathcal{H}+1)]$$

$$\delta^* = \int_o^{\delta} [1-(\rho U)/(\rho_e U_e)]\, dy = (\delta_i^*/\xi)[(1+m_\infty)/(1+m_e)]^{\frac{1}{2}}[Z+1+m_e(\mathcal{H}+1)]$$

$$\theta = \int_o^{\delta} [(\rho U/(\rho_e U_e)]\,[1-(U/U_e)]dy = \delta_i^*(\mathcal{H}/\xi)[(1+m_\infty)/(1+m_e)]^{\frac{1}{2}}$$

$$B = \mathcal{K} + (1+m_e)/m_e \quad ; \quad m_e = (\gamma-1)M_e^2/2$$

$$f = \mathcal{K}\left\{2 + [(\gamma+1)/(\gamma-1)]\, m_e/(1+m_e)\right\} + (3\gamma-1)/(\gamma-1)$$

$$+ Z\,(M_e^2-1)/[m_e(1+m_e)]$$

$$h = (a_\infty/\nu_\infty)\, M_e\, \delta_i^* \left[\frac{(1+m_e)}{m_e(1+m_\infty)}\right] \tan\theta$$

$$C = \frac{(\mu/\mu_\infty)}{(T/T_\infty)} \quad ; \quad \tilde{R}e_{\delta_i^*} = \frac{a_\infty}{\nu_\infty} M_e\, \delta_i^* = \frac{M_e}{M_\infty} Re_{\delta_i^*}$$

$$\beta = \xi\,[(1+m_\infty)/(1+m_e)]^{\frac{1}{2}}$$

A1.2. The Profile Functions

The functions $\mathcal{K}$, J, Z, R and P have been obtained by Klineberg (3) as functions of "a". The table below gives these functions where

$$SYM = C_o + C_1 a + C_2 a^2 + \cdots \quad .$$

ATTACHED PROFILES - ADIABATIC WALL						
Sym	C_0	C_1	C_2	C_3	C_4	C_5
$\mathcal{K}$	.24711	.110560	-.021223	.0043455	-.00097238	.00009921
J	.37372	.169689	-.023356	.0057239	-.00174700	.00019124
Z	1.03539	.483731	-.015025	.0260954	-.00369675	----
R	1.25782	-.555497	.319639	-.0907667	+.01398307	-.00093482
P	---	.487447	-.099274	.0096044	-.00031106	----
$d\mathcal{K}/da$	.11056	-.042447	.013036	-.0038895	.00049603	----
$dJ/d\mathcal{K}$	1.50031	.281050	-.042867	.0026238	----	----

A1.3. The Interaction Equations

A1.3.1. Prandtl-Meyer

$$\theta + \alpha_\omega = - [\nu(M_e) - \nu(M_\infty)]$$

$$\nu(M) = [(\gamma+1)/(\gamma-1)]^{\frac{1}{2}} \tan^{-1} [(M^2-1)(\gamma-1)/\gamma+1)]^{\frac{1}{2}} - \tan^{-1} (M^2-1)^{\frac{1}{2}}$$

$$\xi = \frac{P_e}{P_\infty} = [(1+m_\infty)/(1+m_e)]^{\frac{\gamma}{\gamma-1}}$$

A1.3.2. Tangent-Wedge

$$\theta + \alpha_\omega = \frac{(\xi-1)}{\gamma M_\infty} [\, 1 + (\xi-1)(\gamma+1)/2\gamma \,]^{-\frac{1}{2}}$$

$$\xi = \frac{P_e}{P_\infty} = (m_\infty/m_e)^{\gamma/(\gamma-1)}$$

APPENDIX 2: "STRONG" AND "WEAK" INTERACTION EXPANSIONS

The expansions below are developed by Klineberg (3).

A2.1. Infinite Flat Plate "Weak" Interaction Expansion - Adiabatic

$$a = a_0 + a_1 \bar{\chi} + a_2 \bar{\chi}^2 + \cdots$$

$$M_e/M_\infty = 1 + m_1 \bar{\chi} + m_2 \bar{\chi}^2 + \cdots$$

$$Re_{\delta_i}^*/CM_\infty^3 = \frac{\delta_o}{\bar{\chi}} (1 + \delta_1 \bar{\chi} + \delta_2 \bar{\chi}^2 + \epsilon_2 \bar{\chi}^2 \ln \bar{\chi} + \cdots)$$

where the coefficients are given in the table below for M_∞ equal to 4.0, 6.0, and 8.0

	M_∞		
	4.0	6.0	8.0
δ_0	1.7239	1.7239	1.7239
δ_1	0.3160	0.2980	0.2909
δ_2	0.0658	0.0578	0.0543
ϵ_2	-.02925	-.02466	-.02203
a_0	1.6331	1.6331	1.6331
a_1	0.2878	0.2202	0.1989
a_2	0.1298	0.0718	0.0559
m_1	-.07930	-0.06065	-.05479
m_2	-.003164	+.000496	+.001389

A2.2. "Strong" Interaction Expansion - Adiabatic Wall, Infinite Flat Plate

$$\frac{Re_{\delta_i}^*}{CM_\infty^3} = \frac{1.1944}{\bar{\chi}^{1/(2\gamma)}}\left(1 + 0.9479/\bar{\chi} - 0.1988/\bar{\chi} + \cdots\right)$$

$$a = 2.288 - 1.101/\bar{\chi} + 2.136/\bar{\chi}^2 + \cdots$$

$$\frac{M_e}{M_\infty} = 1.1012\,\bar{\chi}^{-(\gamma-1)/2\gamma}\left(1 - 0.2165/\bar{\chi} + 0.1514/\bar{\chi}^2 + \cdots\right)$$

APPENDIX 3: THE "GENERALIZED" LAMINAR BOUNDARY LAYER EQUATIONS

A3.1. Nomenclature

All quantities below are normalized in the following fashion: r, $(\varkappa)^{-1}$, y, and x with respect to an arbitrary length L; U, V, ρ, T, c_p and μ with their respective undisturbed free stream values; and P with respect to $\rho_\infty U_\infty^2$. $\varkappa$ is the wall curvature; y the normal distance from the surface; and x is coordinate lying along the surface. j = 0 for planar flow and j = 1.0 in the axisymmetric case. θ is the surface inclination relative to the axis of axisymmetry. Further,

$$Re = \frac{\rho_\infty U_\infty L}{\mu_\infty} \quad \text{and} \quad Pr = \frac{c_{p_\infty} \mu_\infty}{k_\infty}$$

Subscript x and y below refer to partial differentiation.

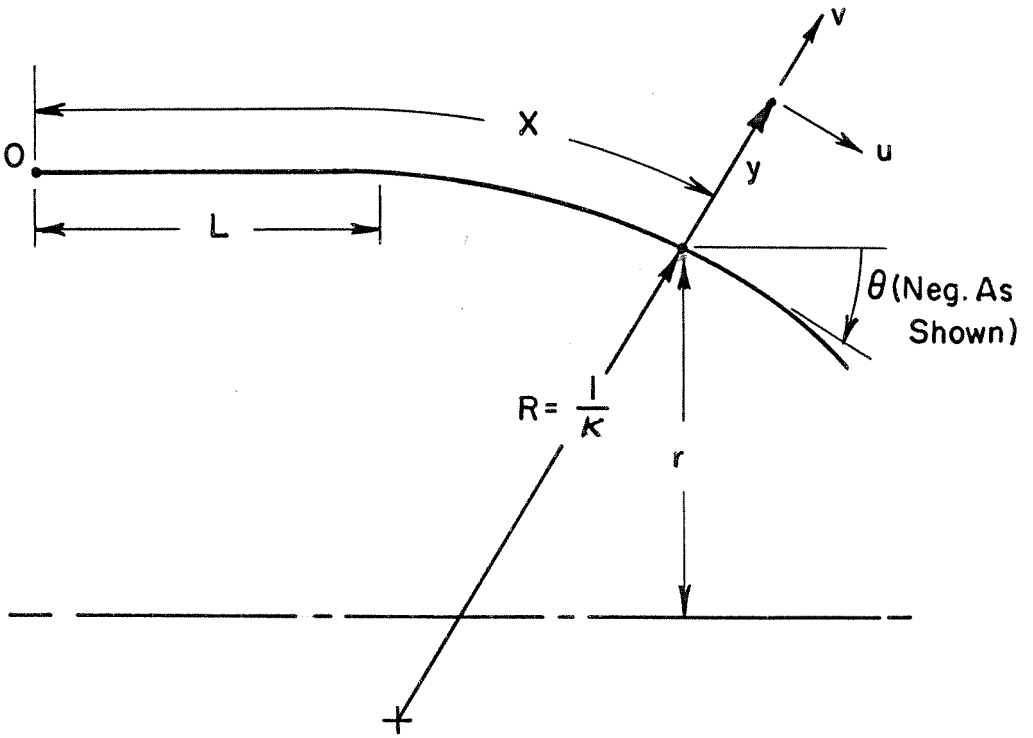

A3.2. Continuity

$$\left[(r + y\cos\theta)^j \rho U\right]_x + \left[(1 + \varkappa y)(r + y\cos\theta)^j \rho V\right]_y = 0$$

A3.3. Longitudinal Momentum

$$\left(\frac{1}{1+\varkappa y}\right)\rho U U_x + \rho V U_y + \left(\frac{\varkappa}{1+\varkappa y}\right)\rho U V$$

$$= -\left(\frac{1}{1+\varkappa y}\right)P_x + \frac{1}{Re}\left\{\left[\mu\left(U_y - \frac{\varkappa U}{1+\varkappa y}\right)\right]_y + \mu\left(\frac{2\varkappa}{1+\varkappa y} + \frac{j\cos\theta}{r+y\cos\theta}\right)\left(U_y - \frac{\varkappa U}{1+\varkappa y}\right)\right\}$$

A3.4. Transverse Momentum

$$\left(\frac{1}{1+\varkappa y}\right)\rho U V_x + \rho V V_y - \left(\frac{\varkappa}{1+\varkappa y}\right)\rho U^2$$

$$= -P_y + \frac{1}{Re}\frac{4}{3}\left[\mu V_y\right]_y$$

A3.5. Energy

$$\left(\frac{1}{1+\varkappa y}\right)\rho U c_p T_x + \rho V c_p T_y$$

$$= (\gamma-1)M_\infty^2\left\{\left(\frac{1}{1+\varkappa y}\right)U P_x + V P_y\right\} + \frac{1}{RePr}\left\{(\mu c_p T_y)_y + \left(\frac{\varkappa}{1+\varkappa y} + \frac{j\cos\theta}{r+y\cos\theta}\right)\mu c_p T_y\right\} + \frac{(\gamma-1)M_\infty^2}{Re}\mu\left(U_y^2 + \frac{4}{3}V_y^2\right)$$

A3.6. State

$$\gamma M_\infty^2 P = \rho T$$

APPENDIX 4: FINITE DIFFERENCE RELATIONS

A4.1. Nomenclature

The sketch below gives a typical mesh point within the boundary layer.

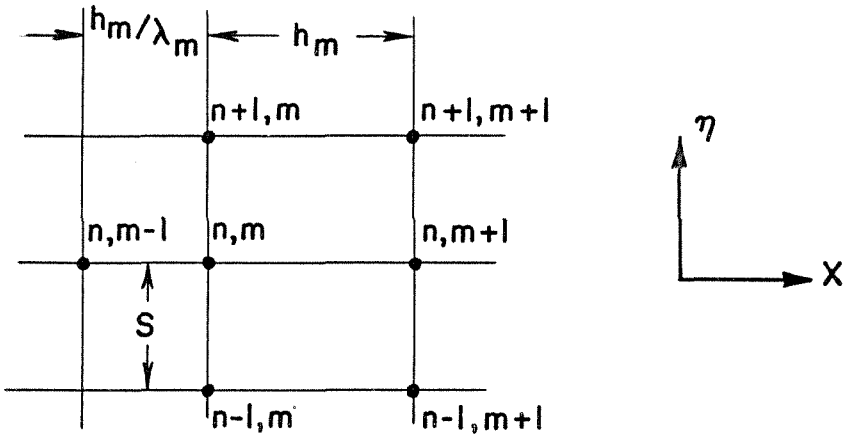

λ is the ratio of step sizes, in the x direction, as indicated above. In the equations that follow (j) refers to the iteration number, $j = 0$ representing the first calculation at the n, m node point. h_m and s are the step sizes in the η and x directions respectively. η is the transformed lateral coordinate corresponding to the general transformation

$$(x, y) \rightarrow x, \quad \eta = F\left(\frac{y}{x^d}\right)$$

where F is an arbitrary but twice differentiable function.

A4.2. $\frac{\partial}{\partial x}$

$$h_m \left.\frac{\partial M}{\partial x}\right|^{j}_{n,m+1} = \frac{\lambda}{\lambda+1}\left(\frac{2\lambda+1}{\lambda} - t\right) M^{j}_{n,m+1}$$

$$- \left[\frac{\lambda^2 + 2\lambda + 1}{\lambda + 1} - \lambda t\right] M_{n,m}$$

$$+ \frac{\lambda^2}{\lambda+1}\,(1-t)\, M_{n,m-1}$$

For $t = 1$ this reduces to $h_m \left.\frac{\partial M}{\partial x}\right|^{j}_{n,m+1} = M^{j}_{n,m+1} - M_{n,m}$; for $t = 0$ the difference formula corresponds to a quadratic fit between the three points.

A4.3. $\frac{\partial}{\partial \eta}$

$$\left.\frac{\partial M}{\partial \eta}\right|^{j}_{n,m+1} = \frac{M^{j}_{n+1,m+1} - M^{j}_{n-1,m+1}}{2S}$$

A4.4. $\frac{\partial^2}{\partial \eta^2}$

$$\left.\frac{\partial^2 M}{\partial \eta^2}\right|^{j}_{n,m+1} = \frac{M^{j}_{n+1,m+1} - 2M^{j}_{n,m+1} + M^{j}_{n-1,m+1}}{S^2}$$

A4.5. $\left(\frac{\partial}{\partial \eta}\right)^2$

$$\left(\frac{\partial M}{\partial \eta}\right)^2 \Bigg|^{j}_{n,m+1} = \frac{\left(M^{(j-1)}_{n+1,m+1} - M^{(j-1)}_{n-1,m+1}\right)}{4\,S^2} \cdot$$

$$\cdot \left[2\left(M^{j}_{n+1,m+1} - M^{j}_{n-1,m+1}\right) - \left(M^{(j-1)}_{n+1,m+1} - M^{(j-1)}_{n-1,m+1}\right)\right]$$

where

$$M^{(-1)}_{n\pm1,\,m+1} \equiv M_{n\pm1,\,m}$$

A4.6. $\left(\frac{\partial}{\partial\eta}\right)\left(\frac{\partial}{\partial\eta}\right)$

$$\left(\frac{\partial M}{\partial\eta}\cdot\frac{\partial T}{\partial\eta}\right)\Bigg|^{j}_{n,\,m+1} = \frac{1}{4S^2}\Big[\left(M^{j}_{n+1,\,m+1}-M^{j}_{n-1,\,m+1}\right)\left(T^{(j-1)}_{n+1,\,m+1}-T^{(j-1)}_{n-1,\,m+1}\right)$$

$$-\left(M^{(j-1)}_{n+1,\,m+1}-M^{(j-1)}_{n-1,\,m+1}\right)\left(T^{(j-1)}_{n+1,\,m+1}-T^{(j-1)}_{n-1,\,m+1}\right)$$

$$+\left(M^{(j-1)}_{n+1,\,m+1}-M^{(j-1)}_{n-1,\,m+1}\right)\left(T^{j}_{n+1,\,m+1}-T^{j}_{n-1,\,m+1}\right)\Big]$$

A4.7. $\frac{\partial}{\partial\eta}$ at "Outer Edge"

The continuity equation requires the evaluation of the first partial $\frac{\partial}{\partial\eta}$ at the edge node $n = N$. The mesh appropriate for this calculation is given below:

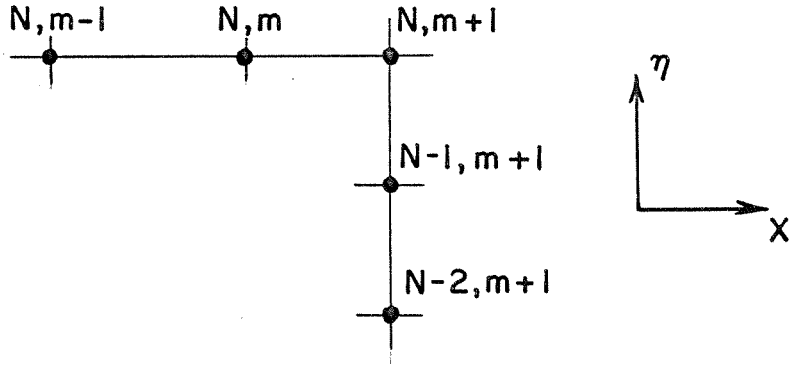

A quadratic fit is used to estimate $\frac{\partial}{\partial \eta}$, i. e.

$$\left.\frac{\partial M}{\partial \eta}\right|^{j}_{N, m+1} = \frac{3}{2S} M^{j}_{N, m+1} - \frac{2}{S} M^{j}_{N-1, m+1} + \frac{1}{2S} M^{j}_{N-2, m+1}$$

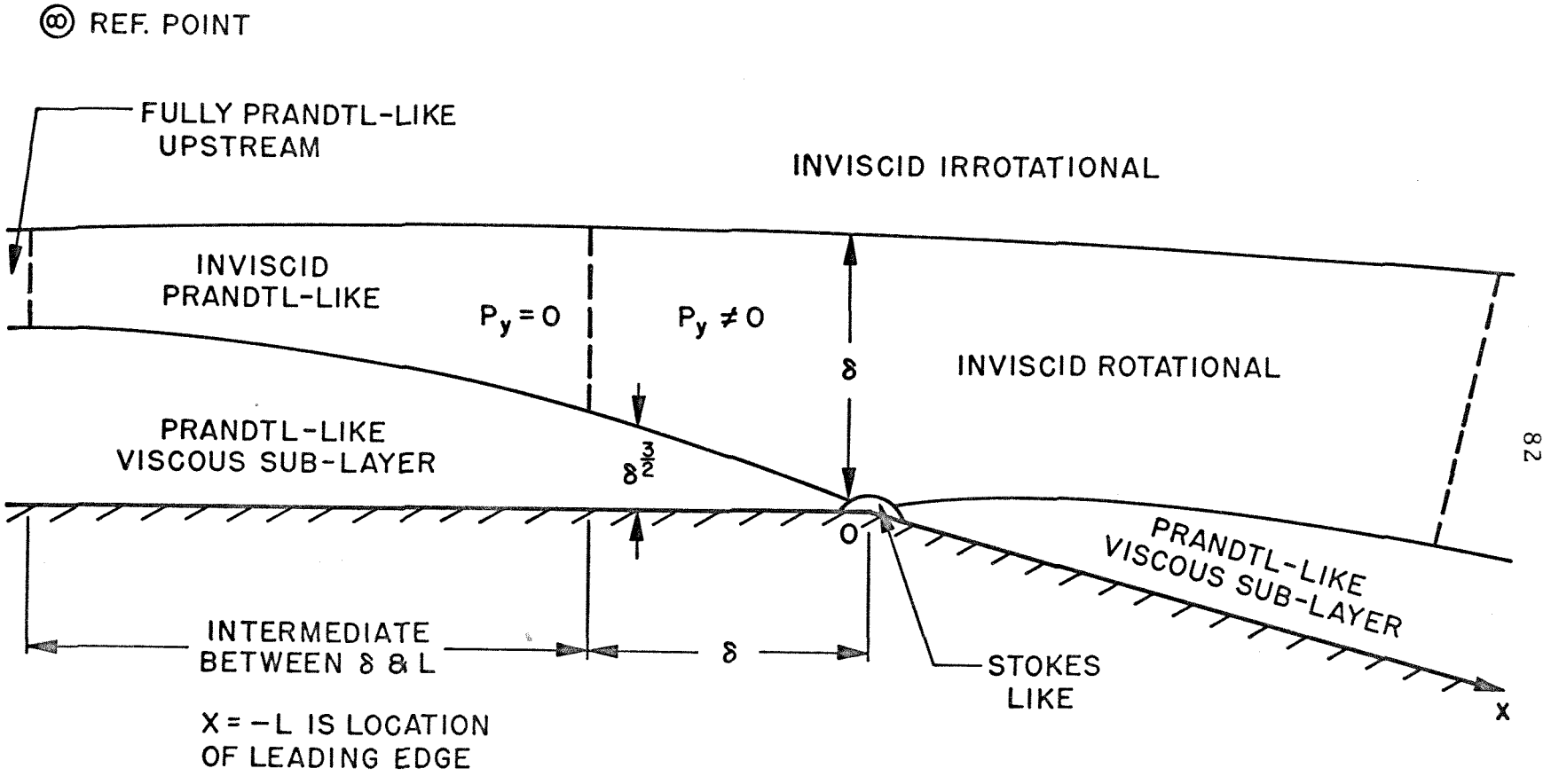

Fig. 1 SCHEMATIC OF CORNER EXPANSION INDICATING THE CHARACTER OF VARIOUS REGIONS

SCHEMATIC OF
"RELAXATION" SURFACE

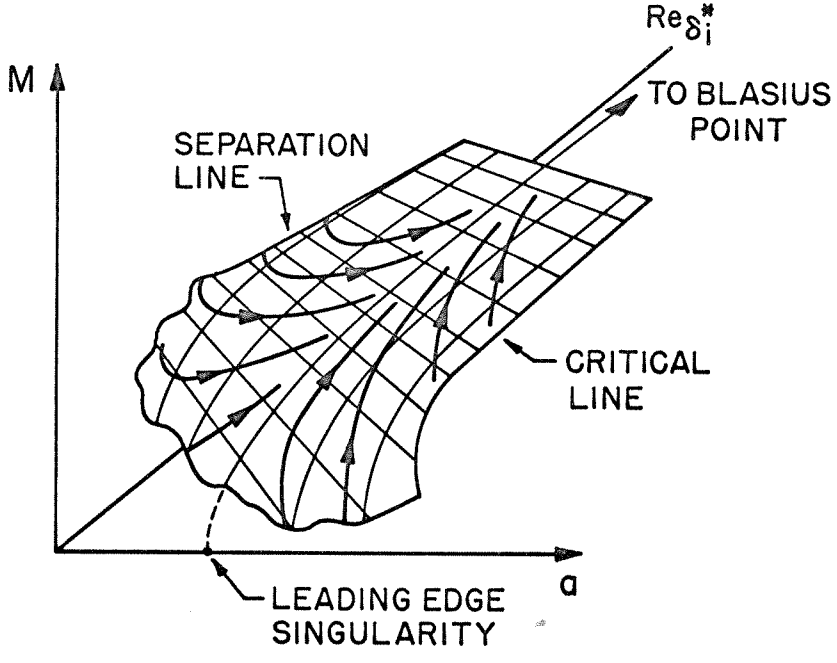

Fig. 2

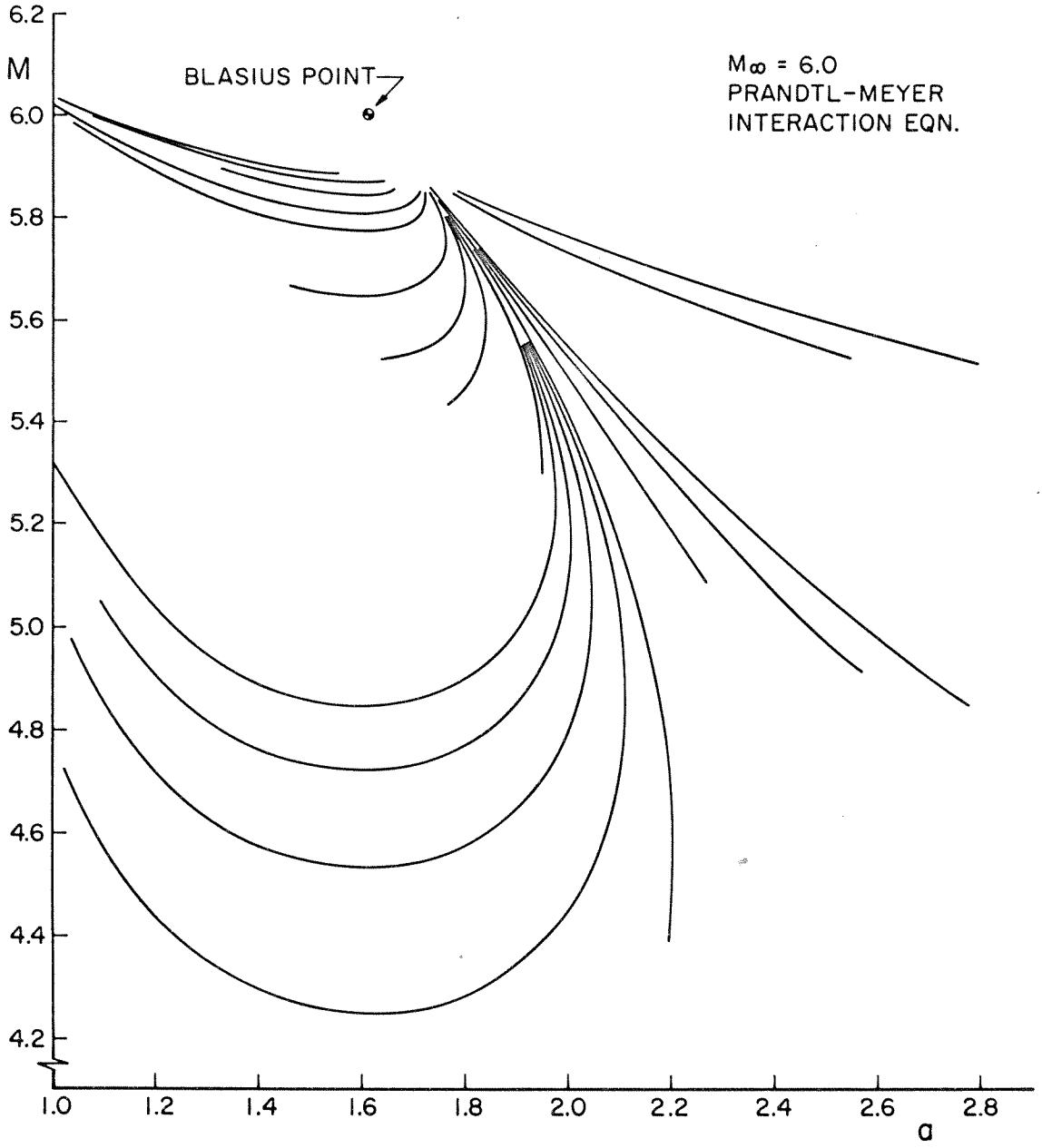

Fig. 3 BLASIUS POINT PHASE SPACE TRAJECTORIES M-a PROJECTION

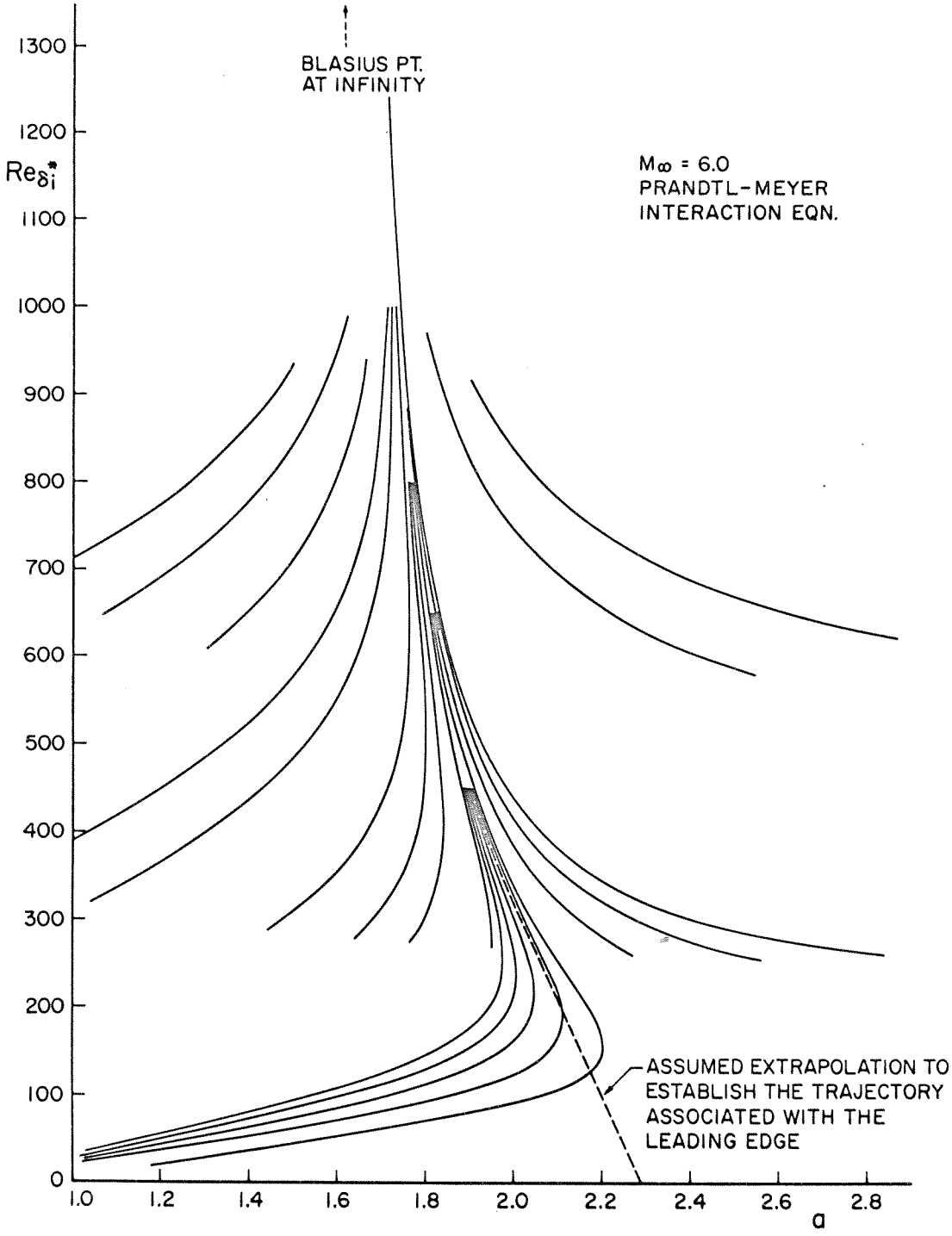

Fig. 4 BLASIUS POINT PHASE SPACE TRAJECTORIES $Re_{\delta_i^*}$-a PROJECTION

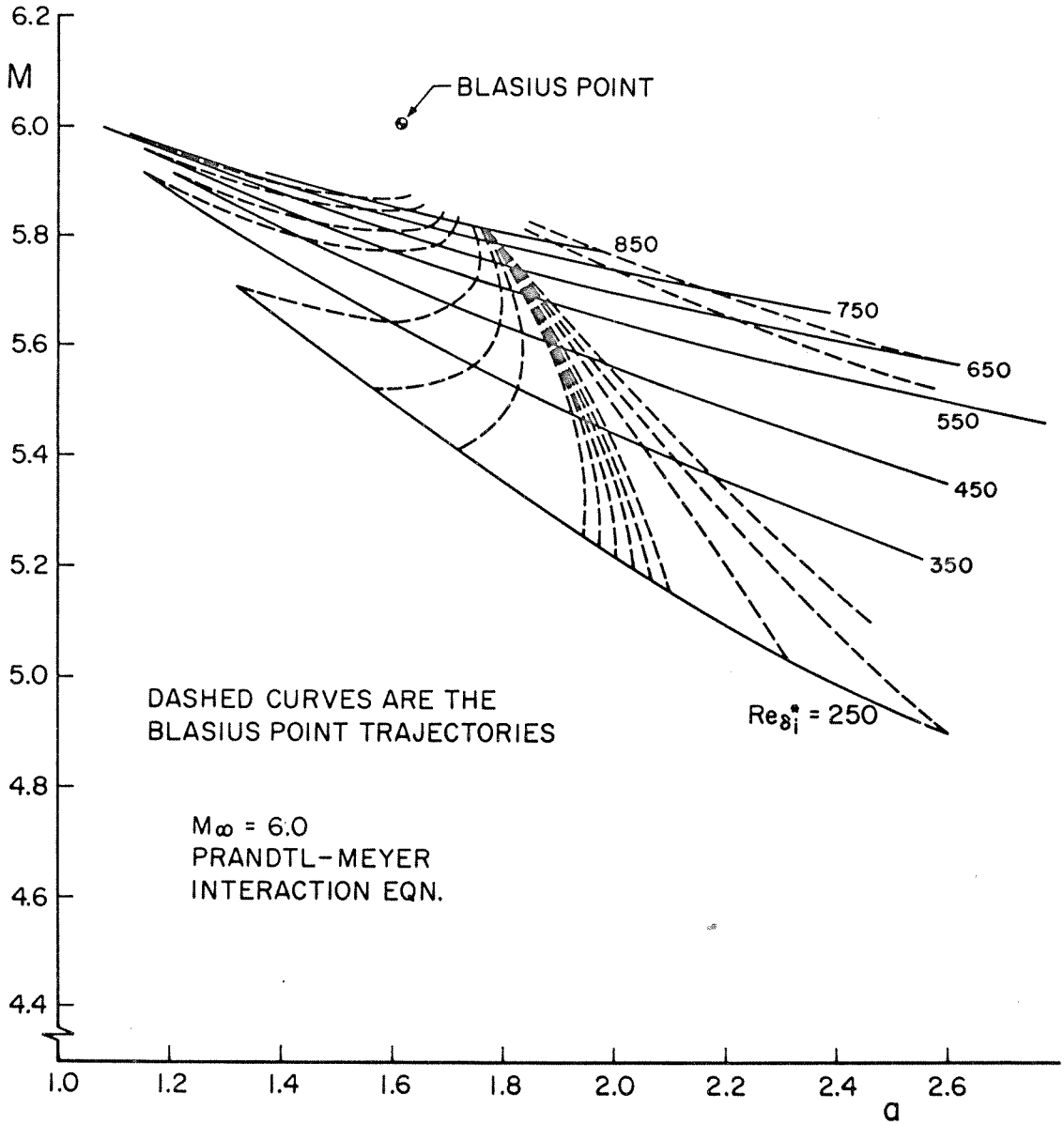

Fig. 5 LEVEL CURVES OF THE RELAXATION SURFACE FOR CONSTANT VALUES OF $Re^*_{\delta_i}$

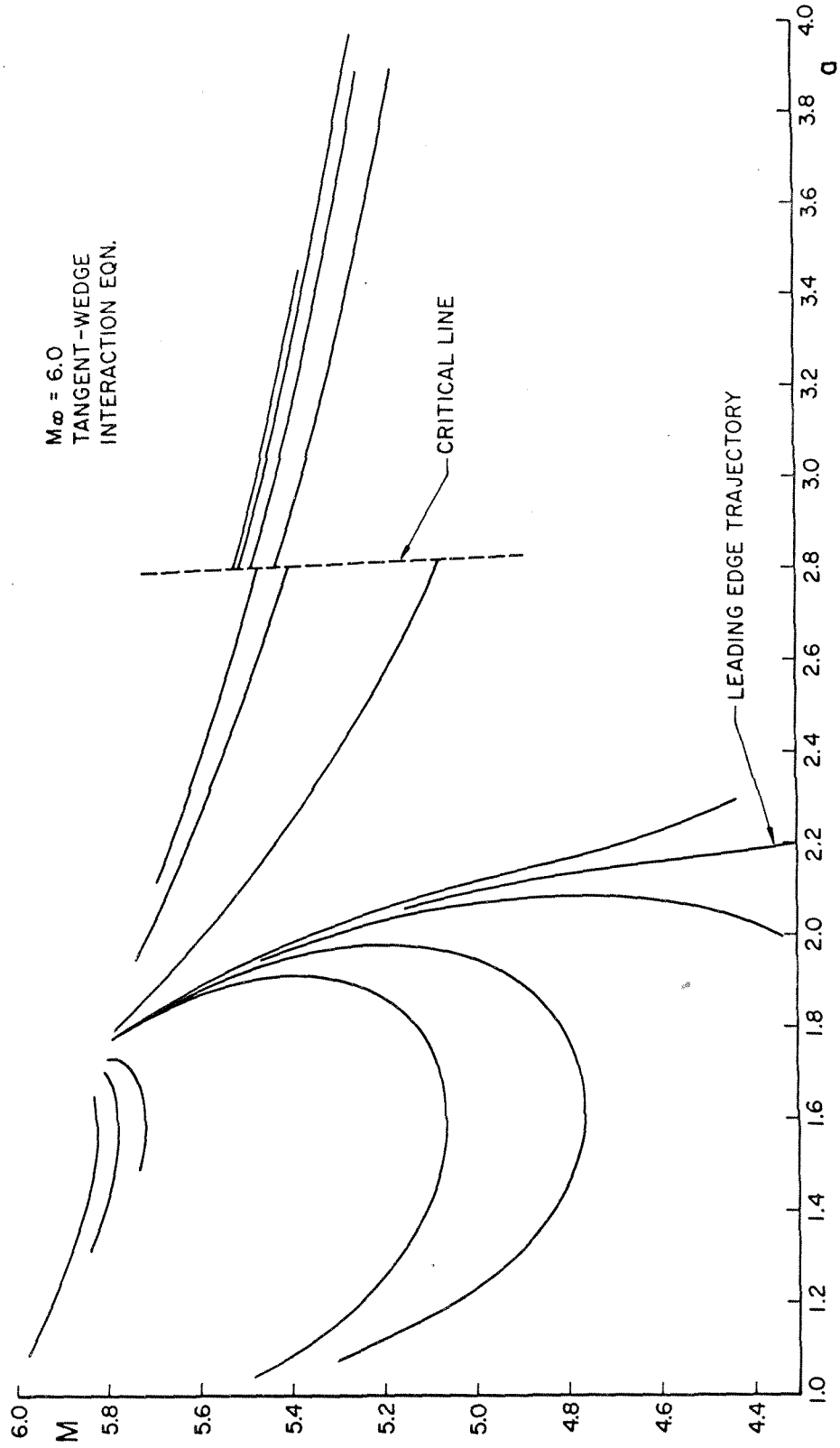

Fig. 6 BLASIUS POINT SPACE TRAJECTORIES M-α PROJECTION

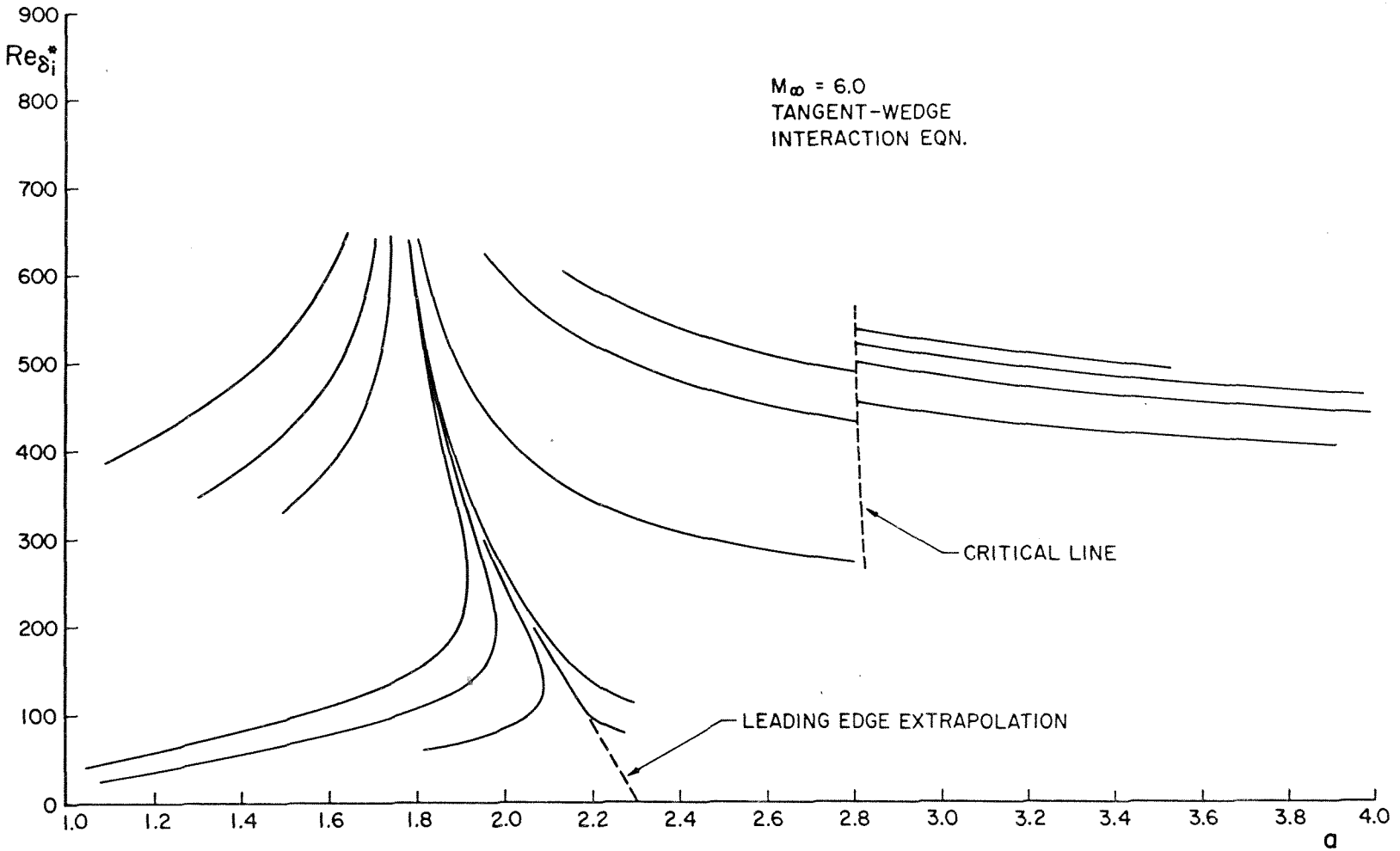

Fig. 7 BLASIUS POINT PHASE SPACE TRAJECTORIES $Re_{\delta_i^*}$-a PROJECTION

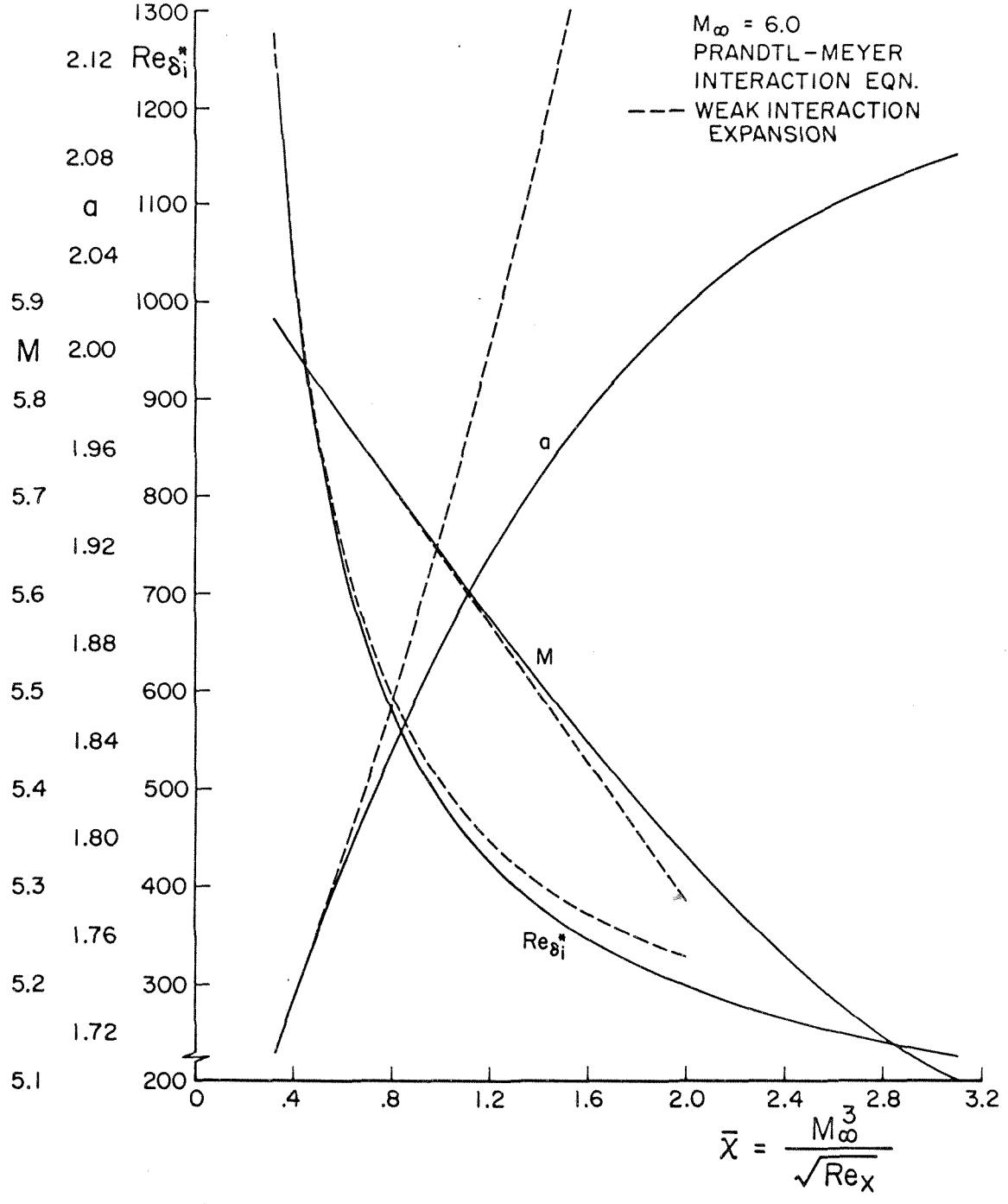

Fig. 8 INFINITE FLAT PLATE MOMENT METHOD SOLUTION

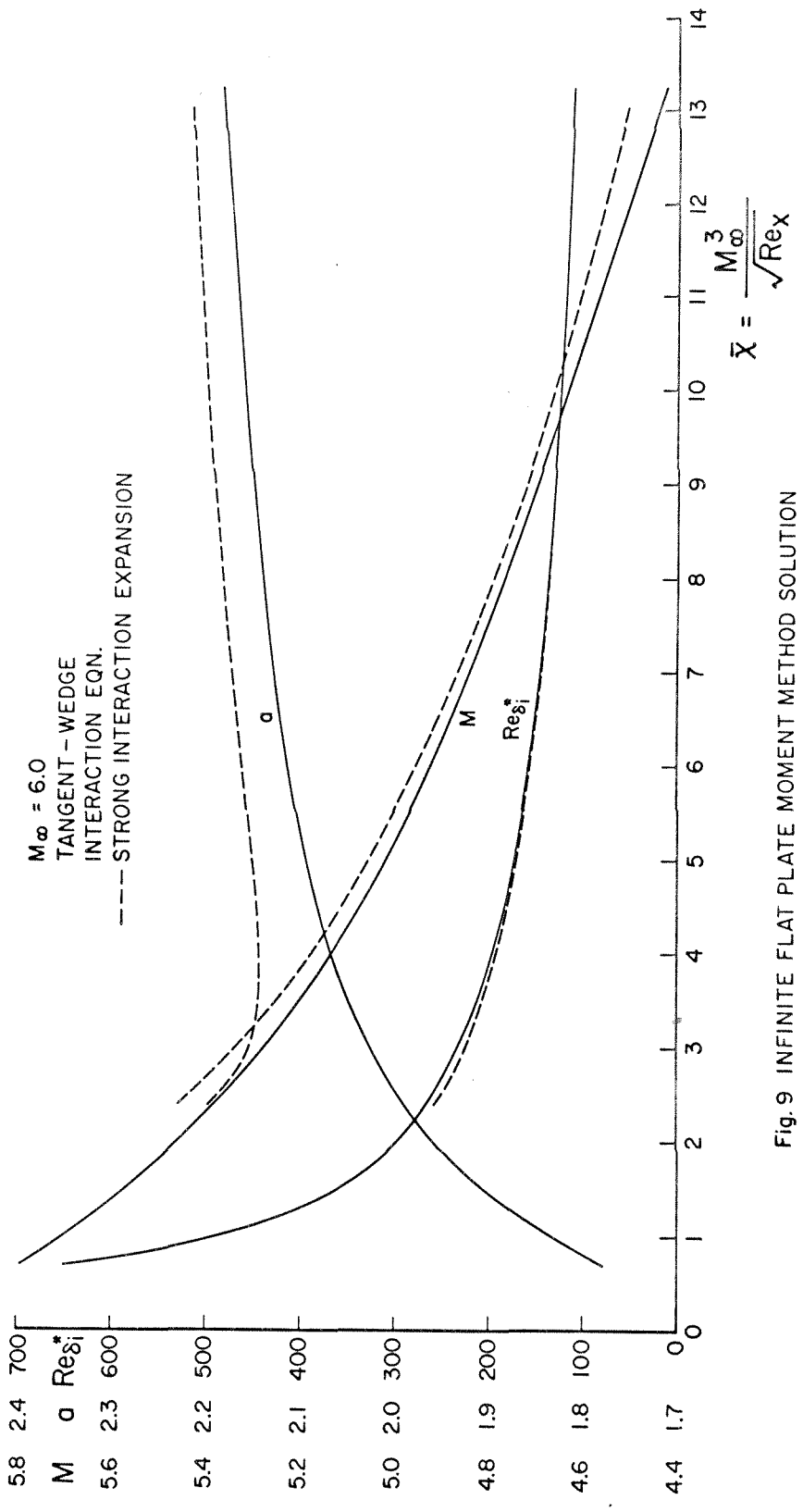

Fig. 9 INFINITE FLAT PLATE MOMENT METHOD SOLUTION

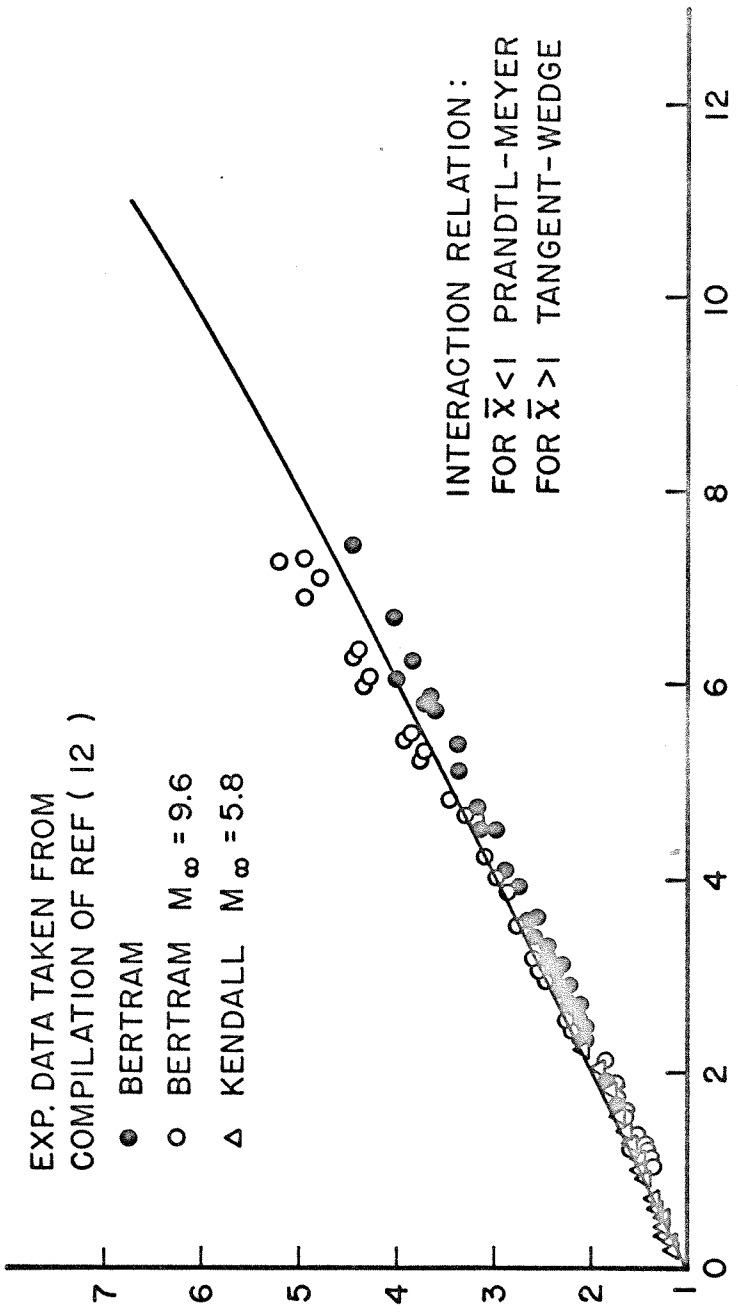

Fig. 10 MOMENT METHOD PREDICTION OF INSULATED FLAT PLATE INTERACTION PRESSURE AND COMPARISON WITH EXPERIMENTAL RESULTS

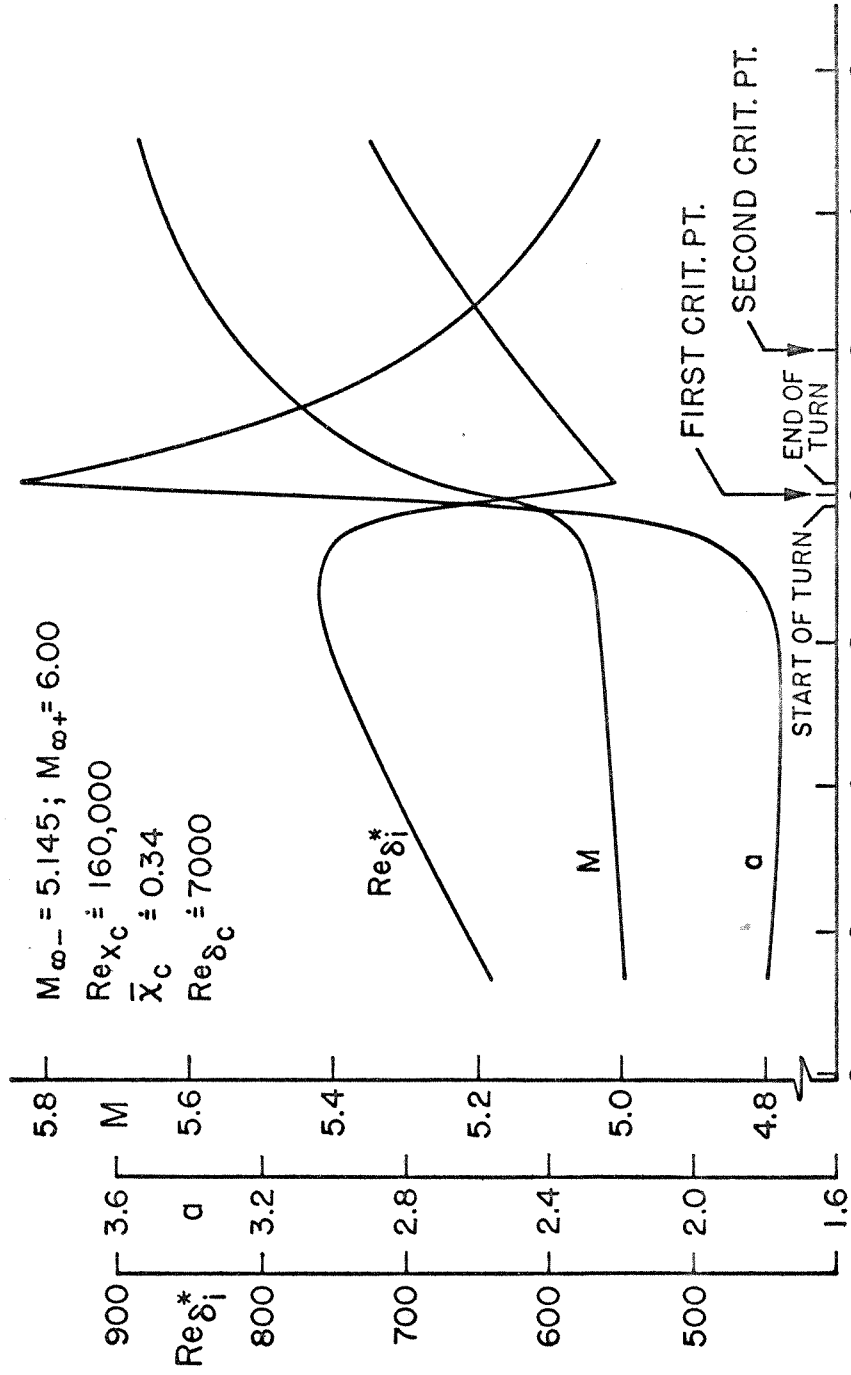

Fig. 11 MOMENT METHOD SOLUTION FOR EXPANSIVE CORNER FLOW.

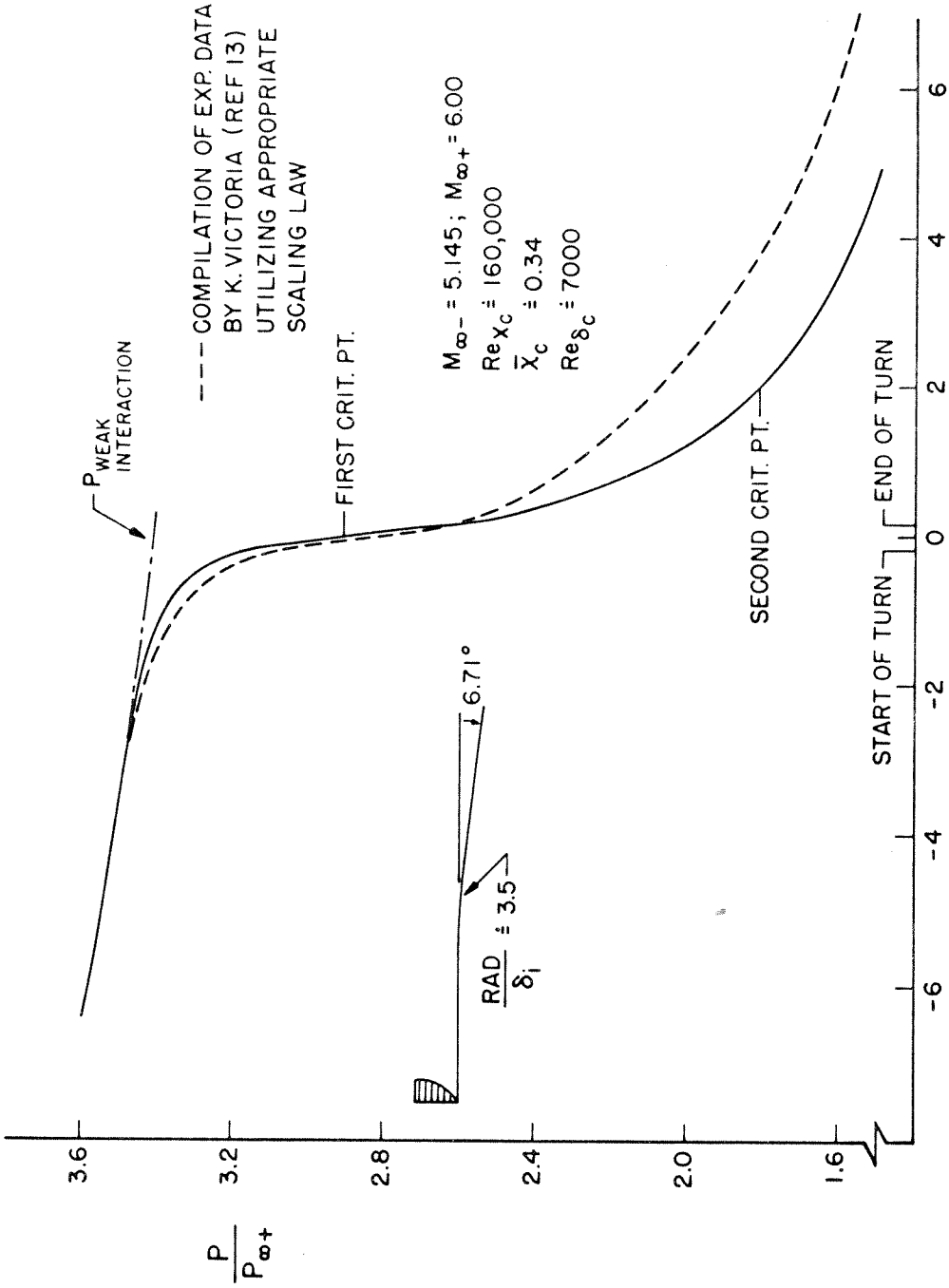

Fig. 12 MOMENT METHOD SOLUTION FOR EXPANSIVE CORNER FLOW.

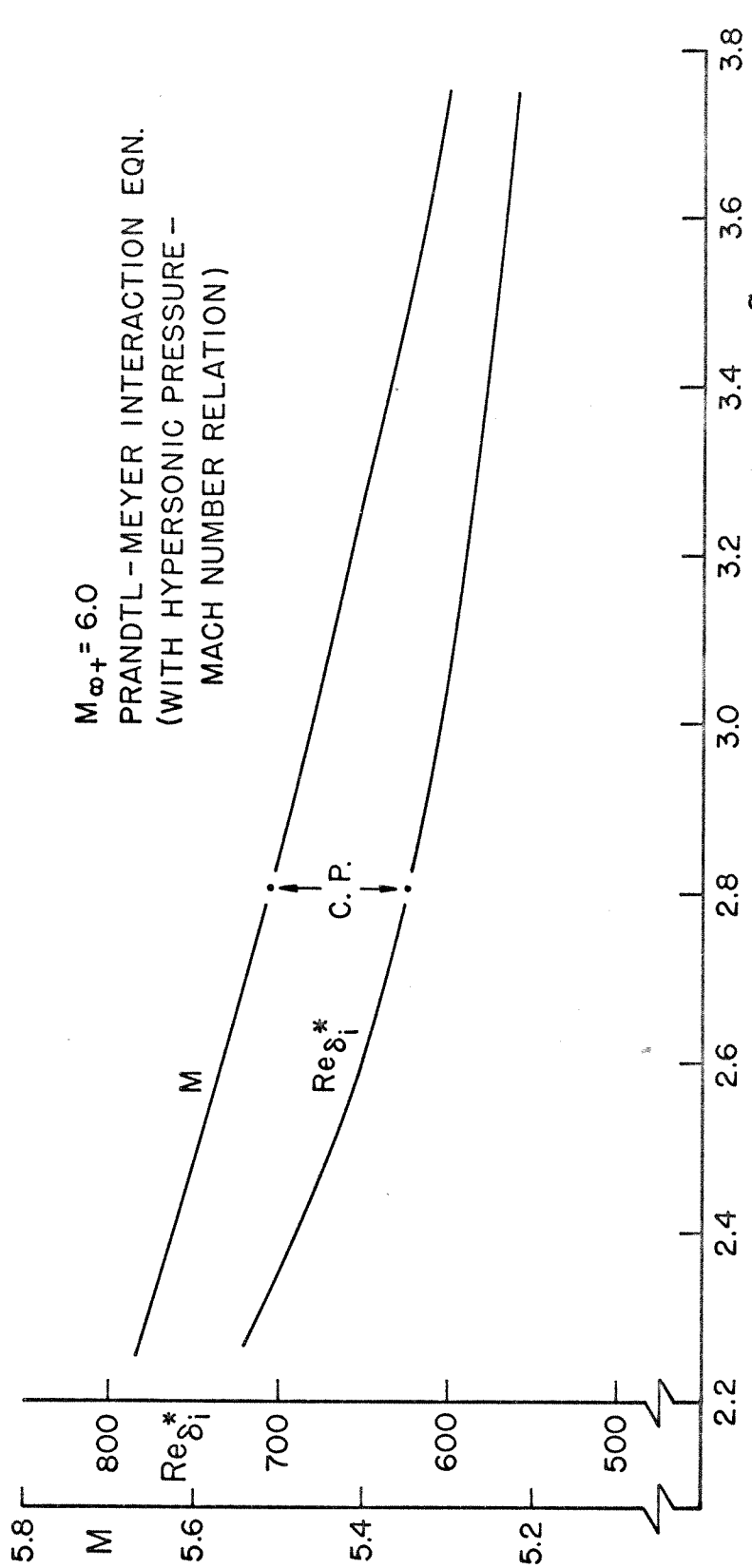

Fig. 13 PHASE SPACE TRAJECTORY THROUGH SECOND CRITICAL POINT FOR EXPANSIVE CORNER FLOW.

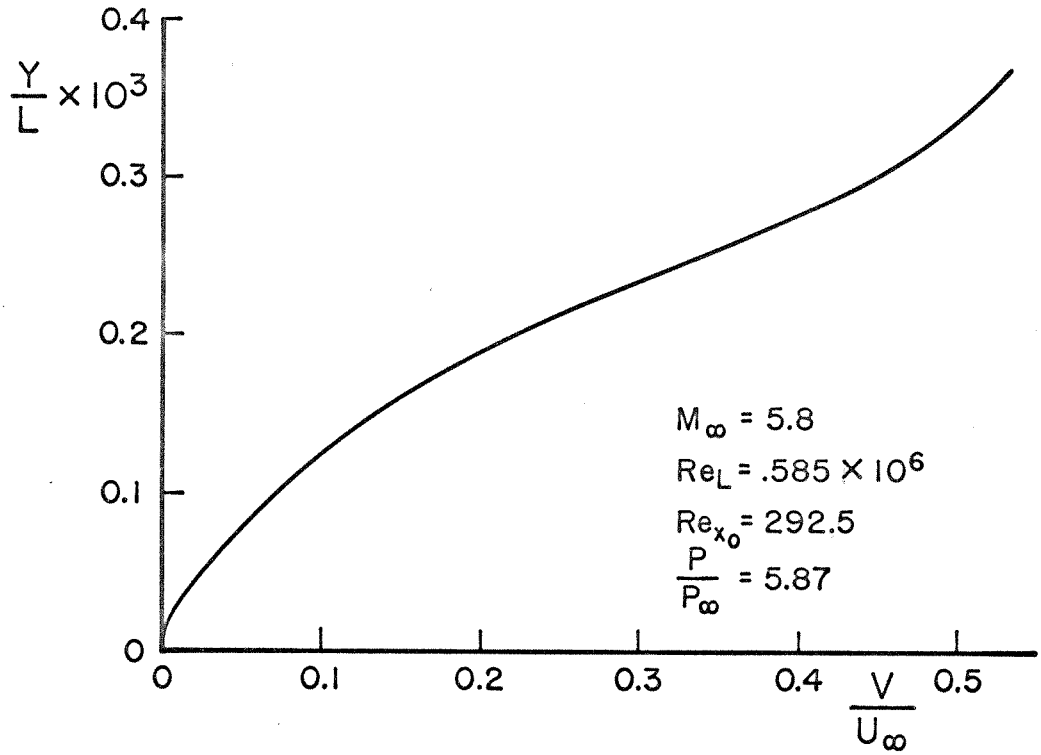

Fig. 15 INITIAL PROFILE NEAR LEADING EDGE

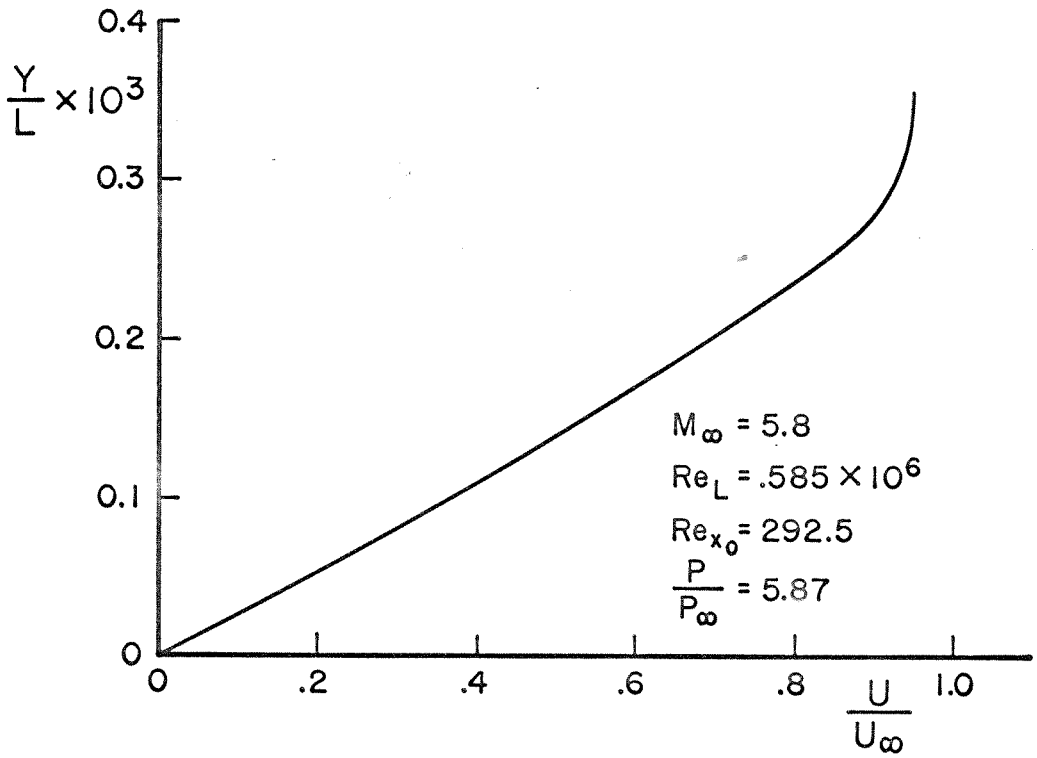

Fig. 14 INITIAL PROFILE NEAR LEADING EDGE

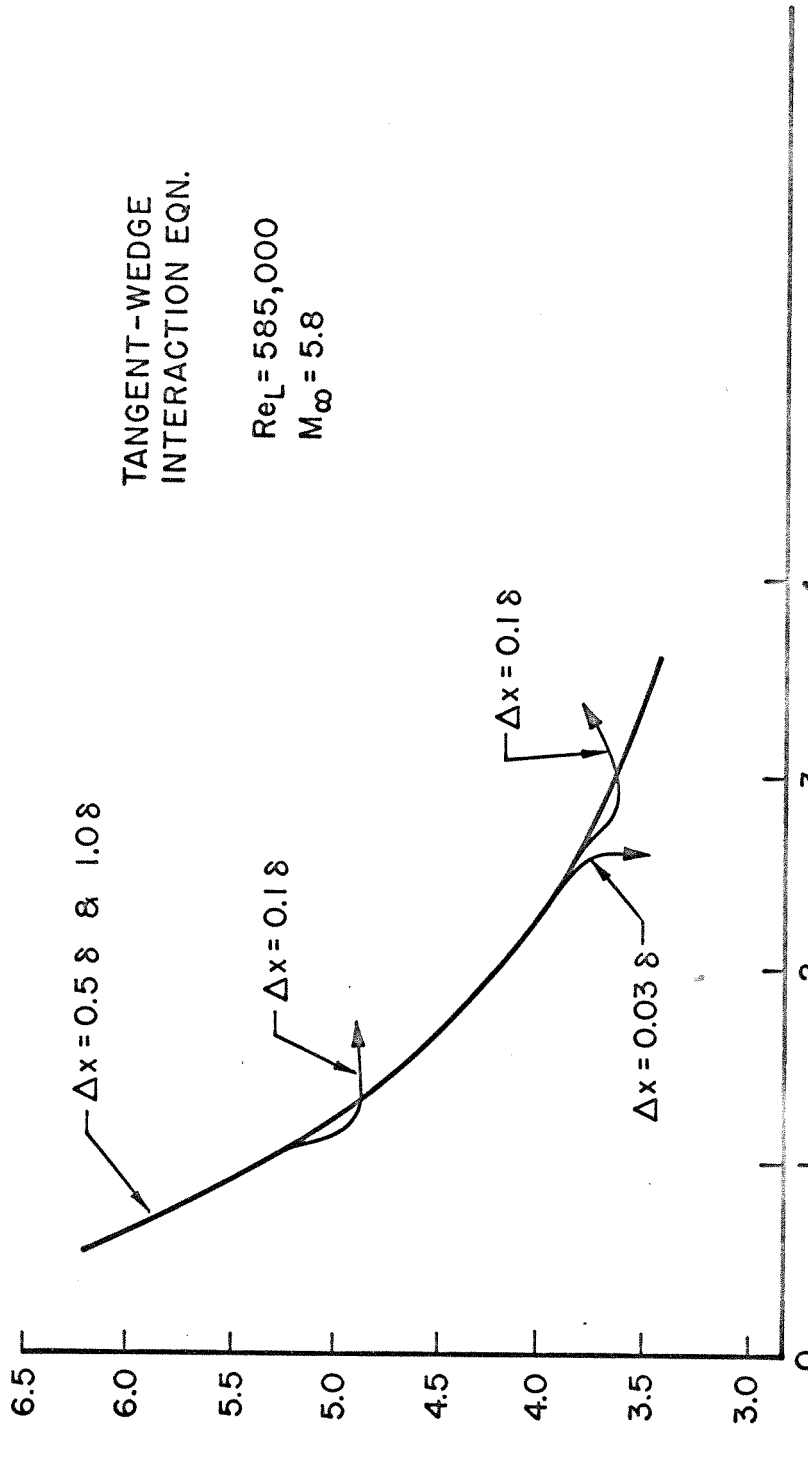

Fig.16 LEADING EDGE PRESSURE DISTRIBUTION - EFFECT OF STEP SIZE IN x

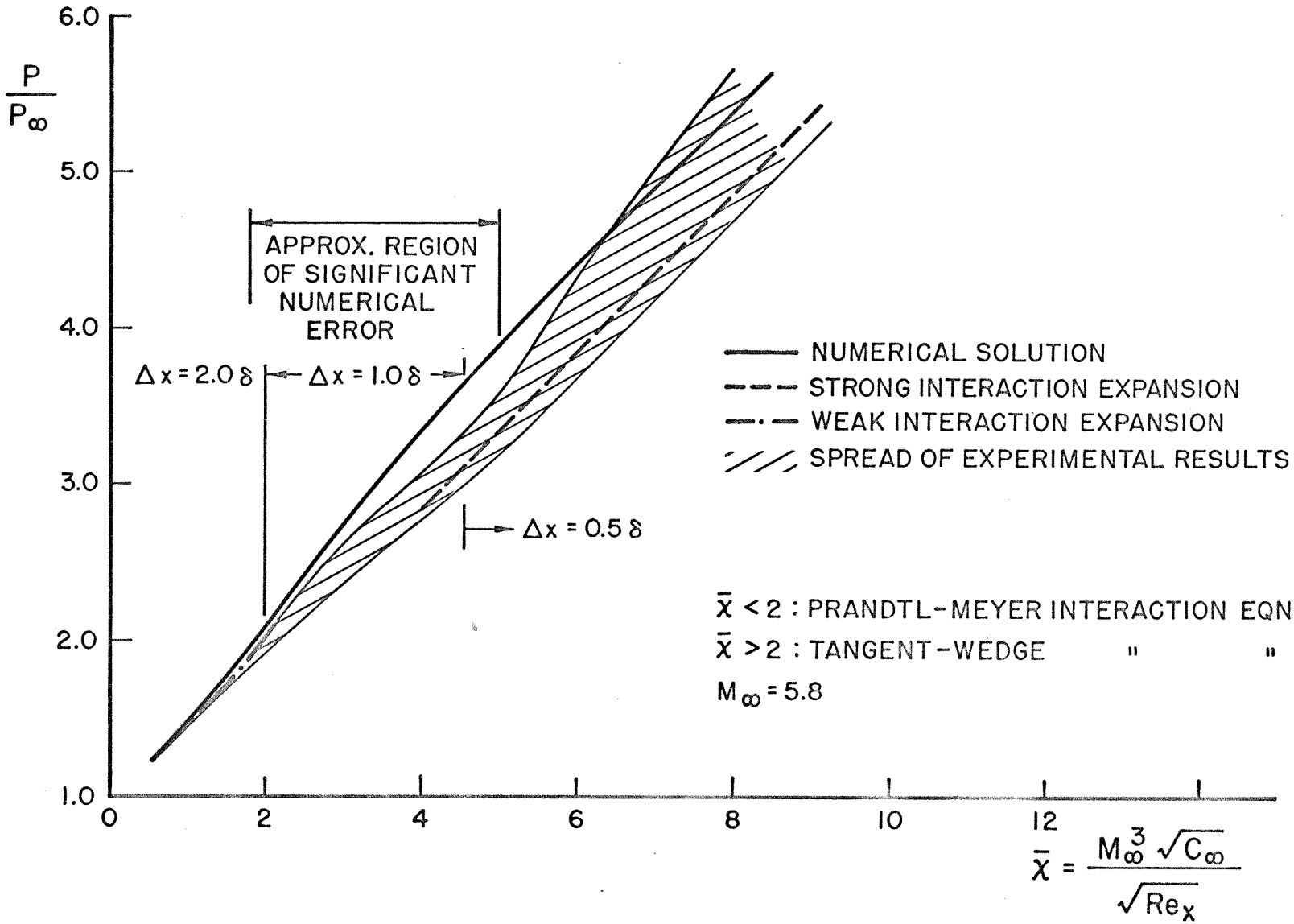

Fig. 17 INFINITE PLATE PRESSURE DISTRIBUTION

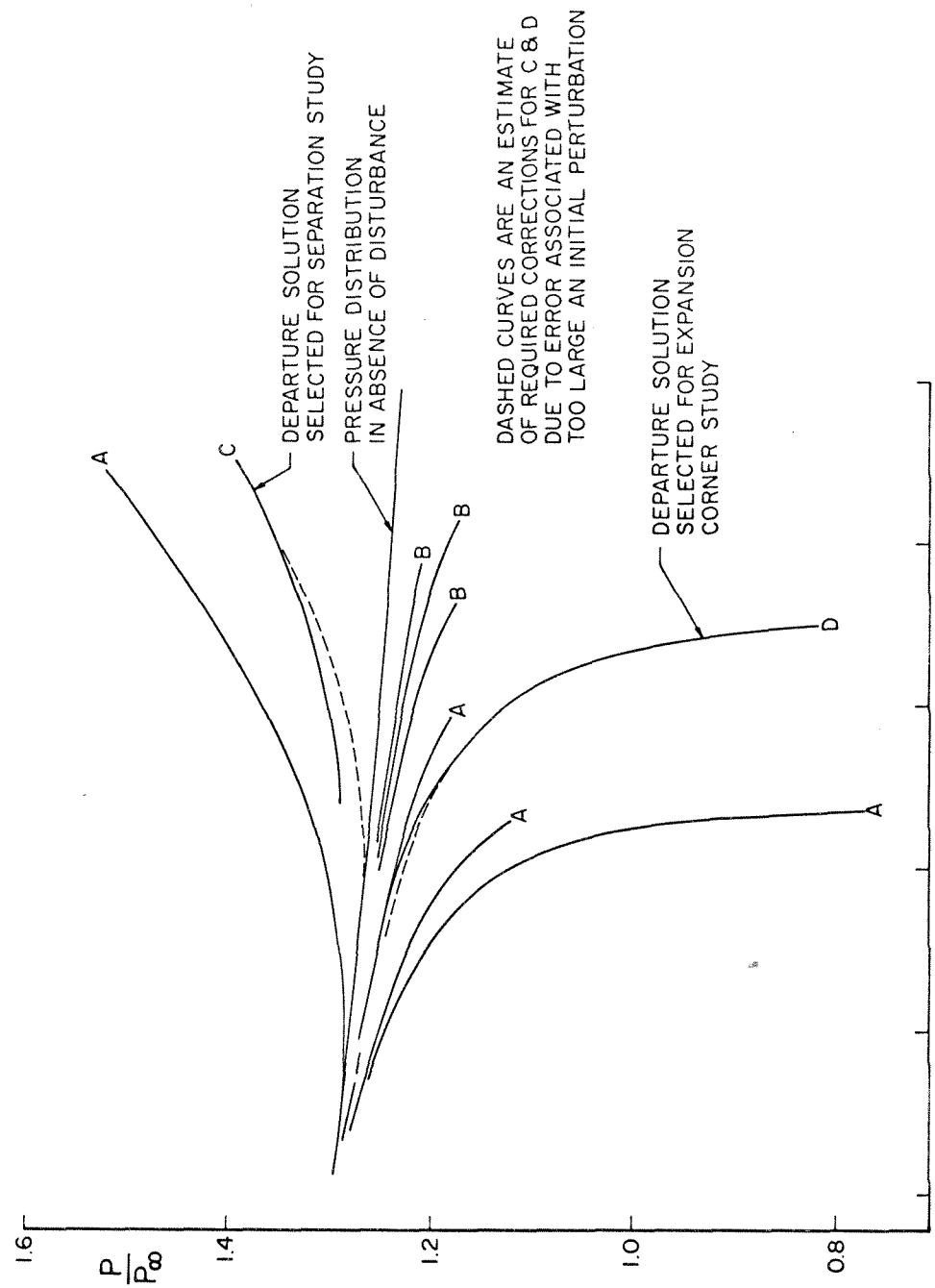

FIG. 18 UPSTREAM INTERACTION DEPARTURES FROM THE INFINITE FLAT PLATE SOLUTION

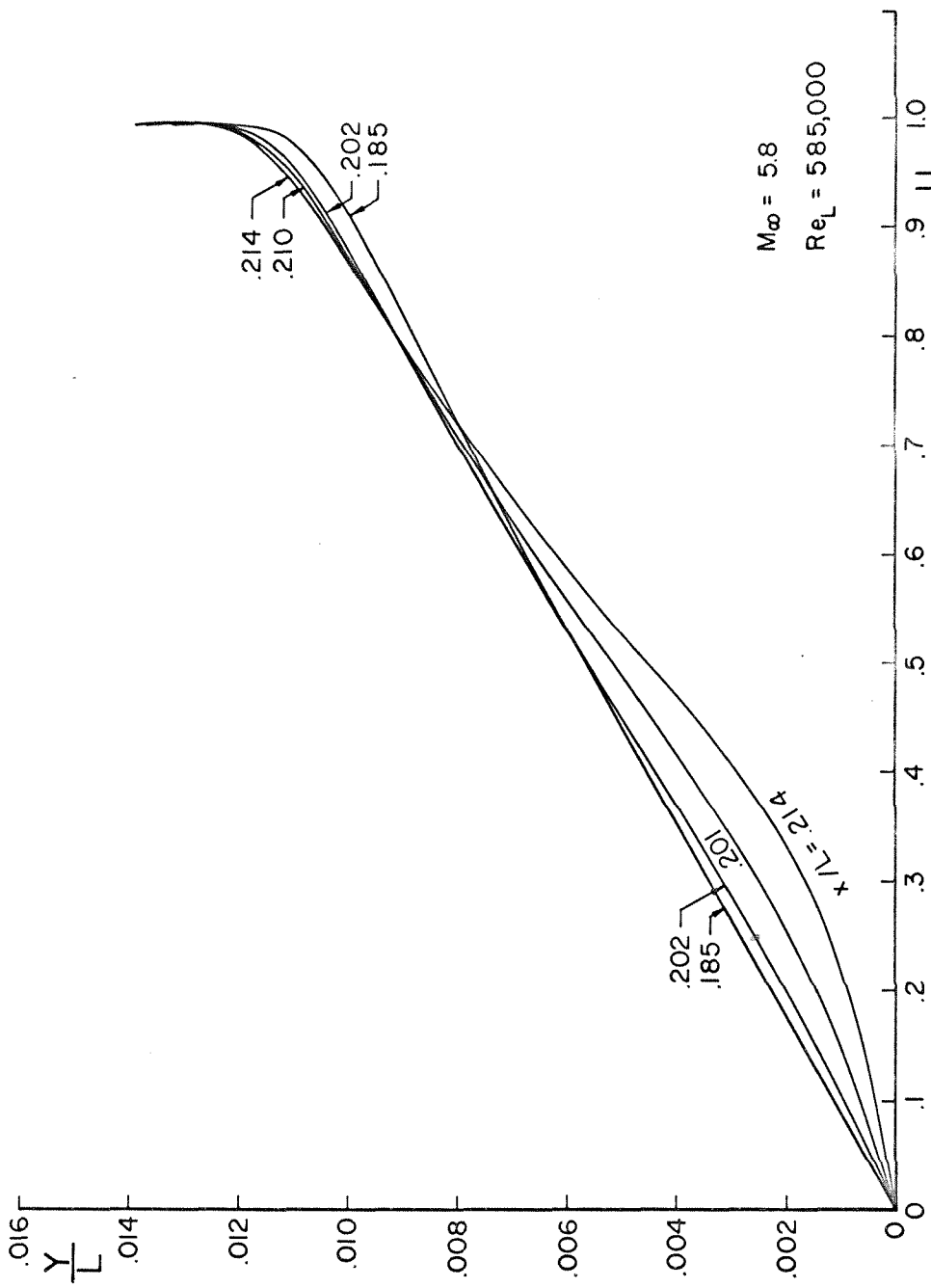

FIG. 19 U-VELOCITY PROFILES FOR EXPANSIVE FREE INTERACTION

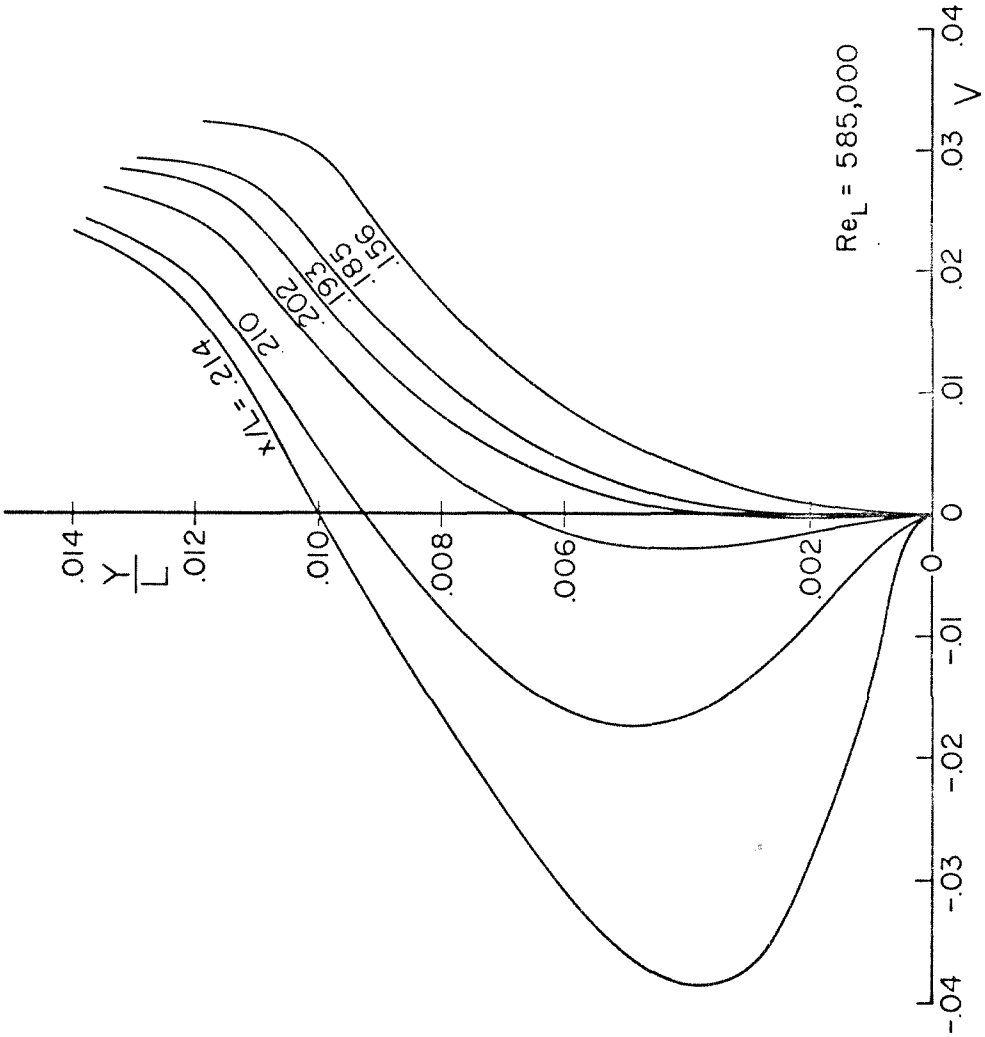

FIG. 20 V-VELOCITY PROFILES FOR EXPANSIVE FREE INTERACTION

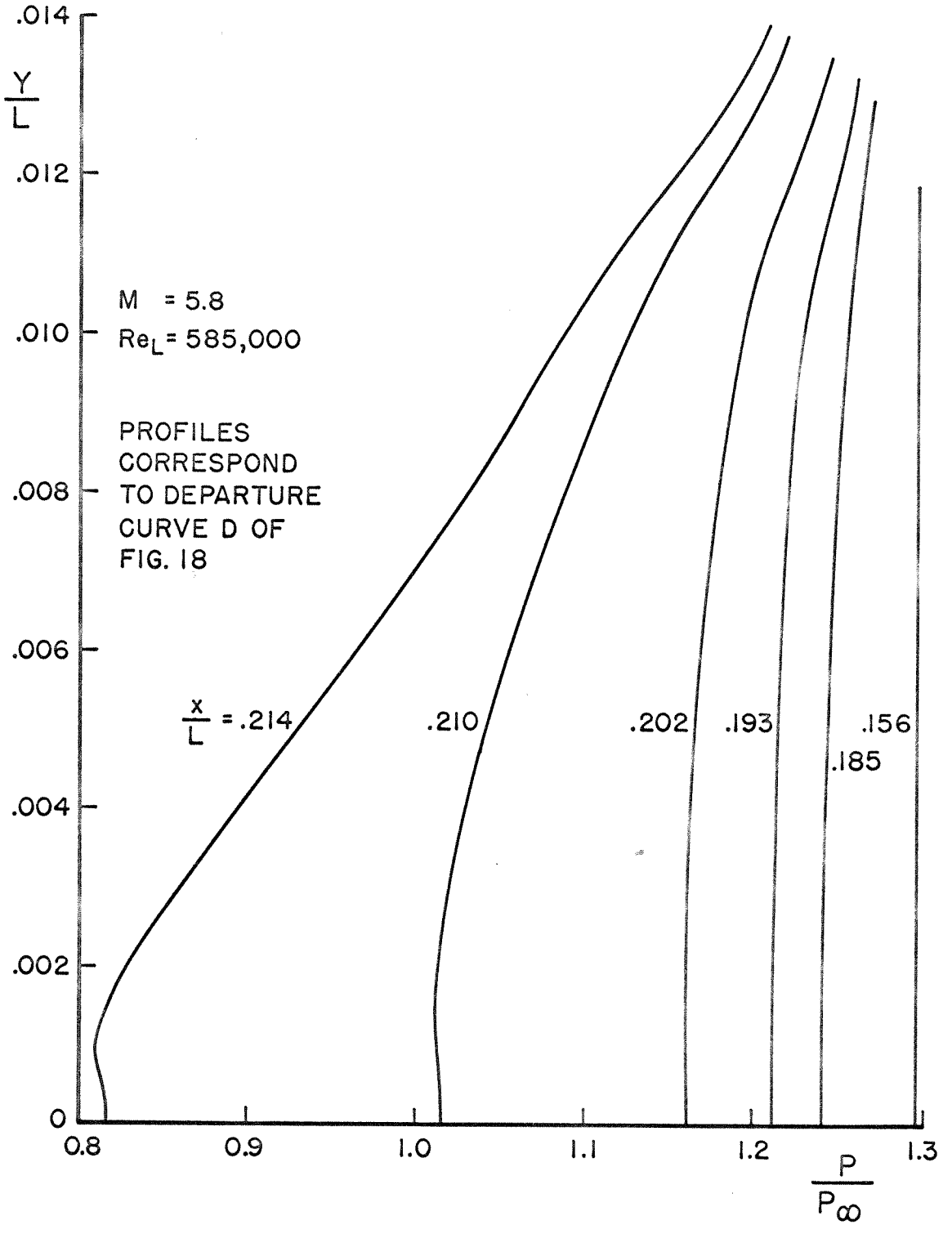

Fig. 21 FREE INTERACTION-EXPANSIVE PRESSURE PROFILES

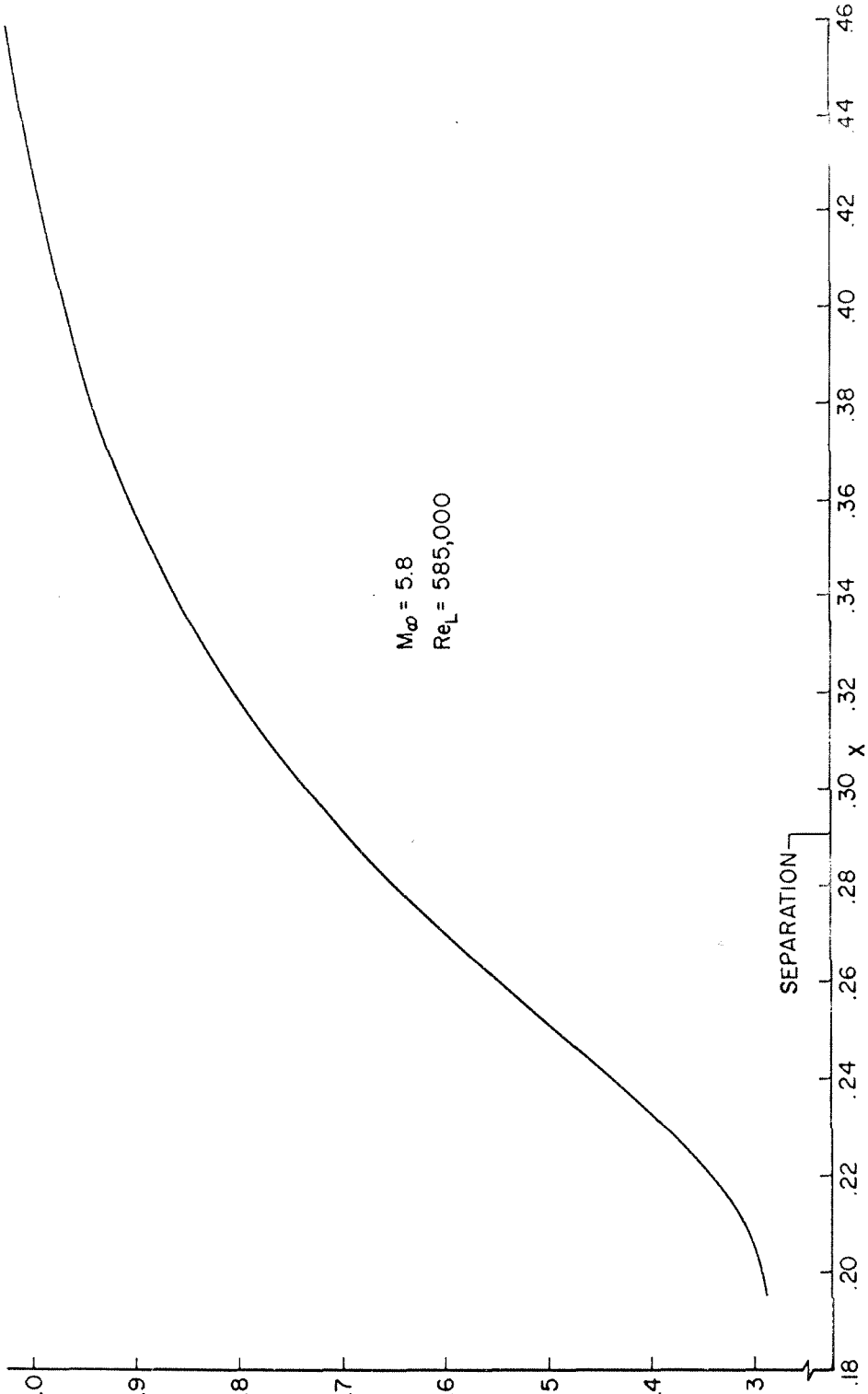

FIG.22 COMPRESSIVE FREE INTERACTION PRESSURE DISTRIBUTION

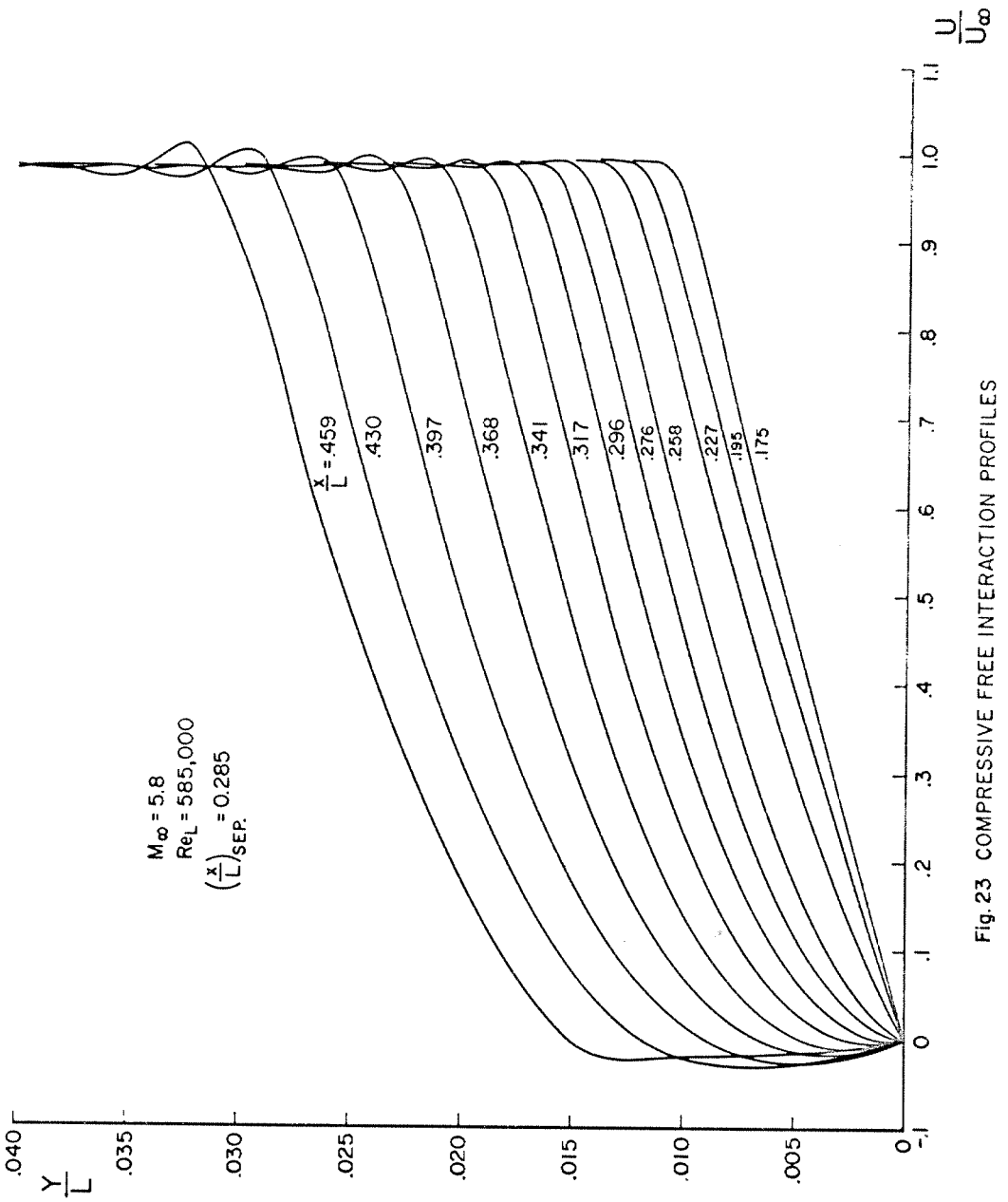

Fig. 23 COMPRESSIVE FREE INTERACTION PROFILES

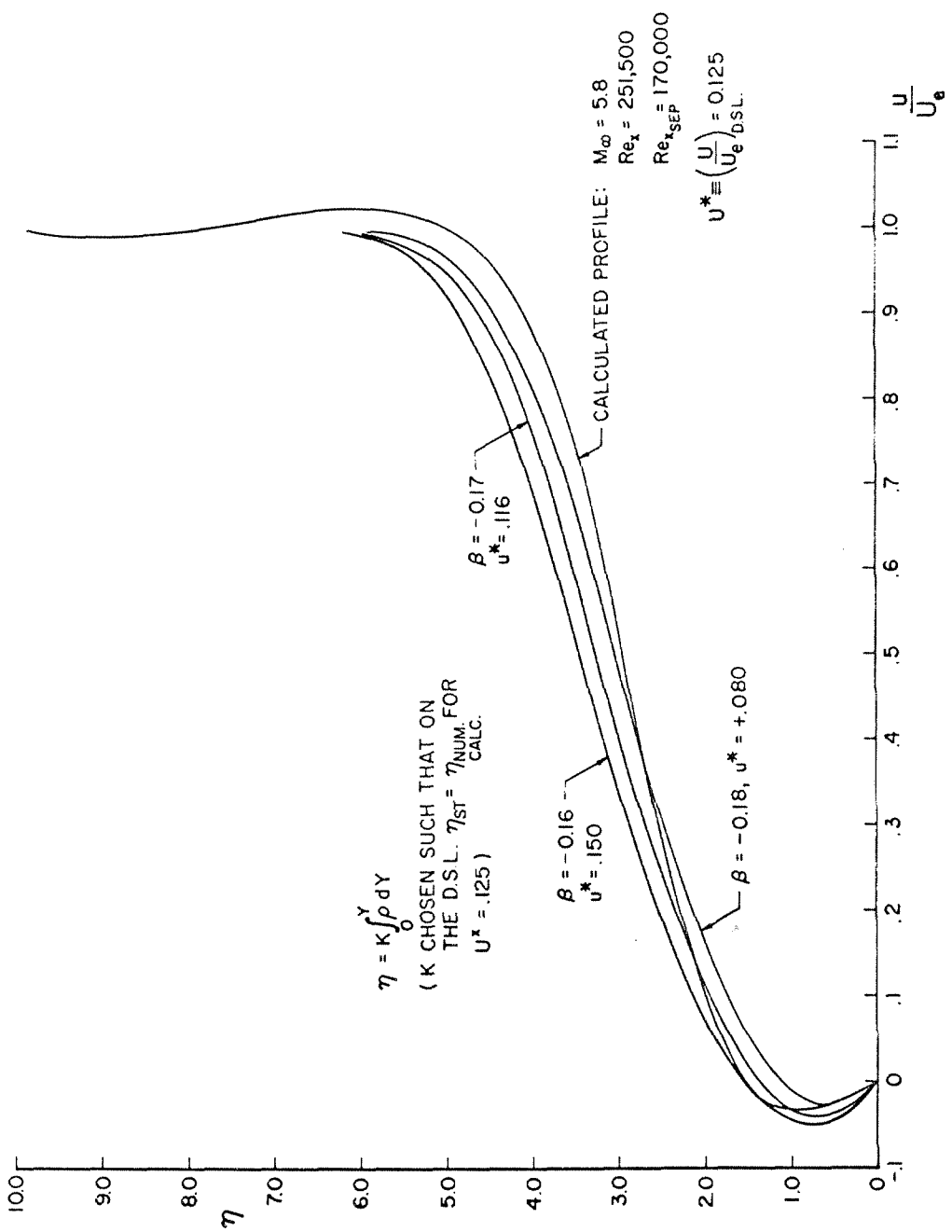

FIG.24 COMPARISON OF A TYPICAL FREE INTERACTION SEPARATED VELOCITY PROFILE WITH THE STEWARTSON SIMILITUDE SOLUTIONS

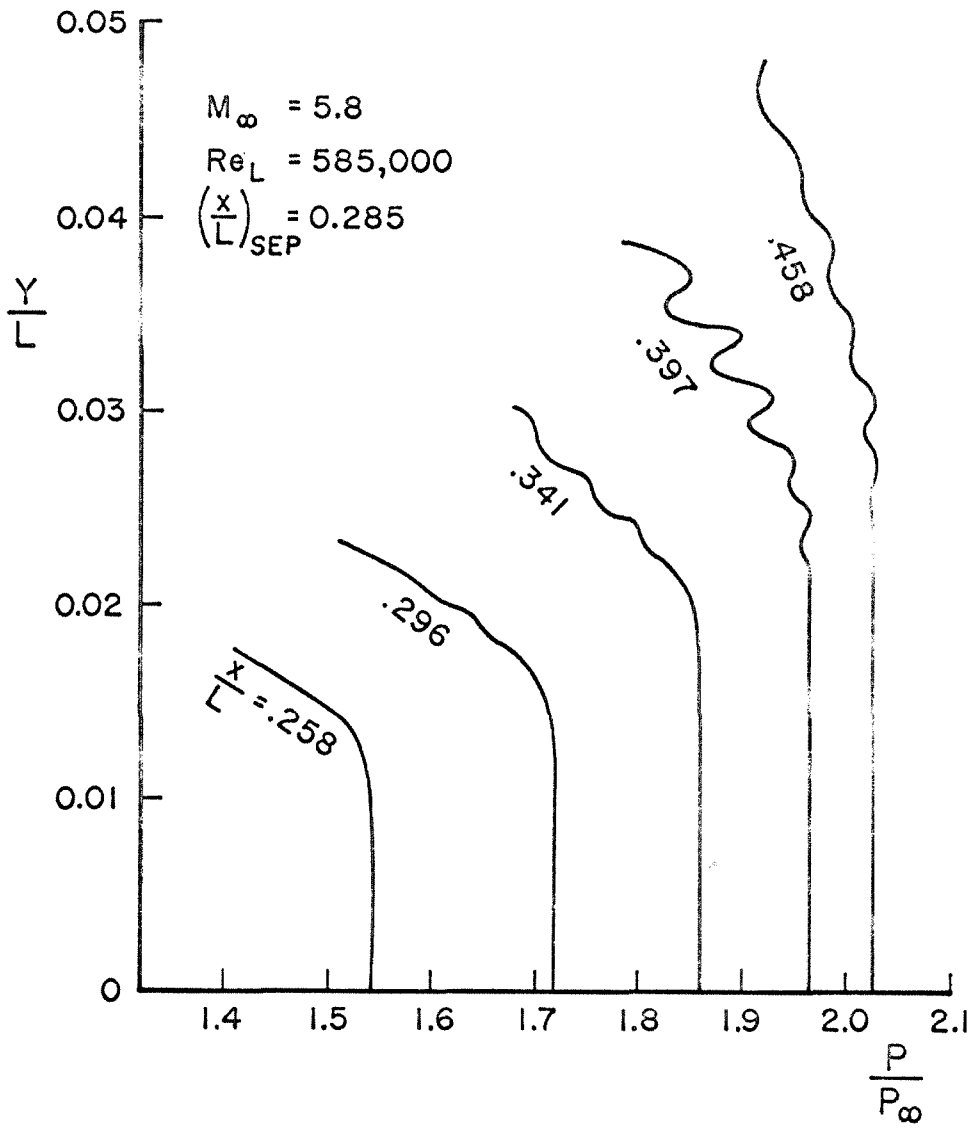

Fig. 25 COMPRESSIVE FREE INTERACTION-PRESSURE PROFILES

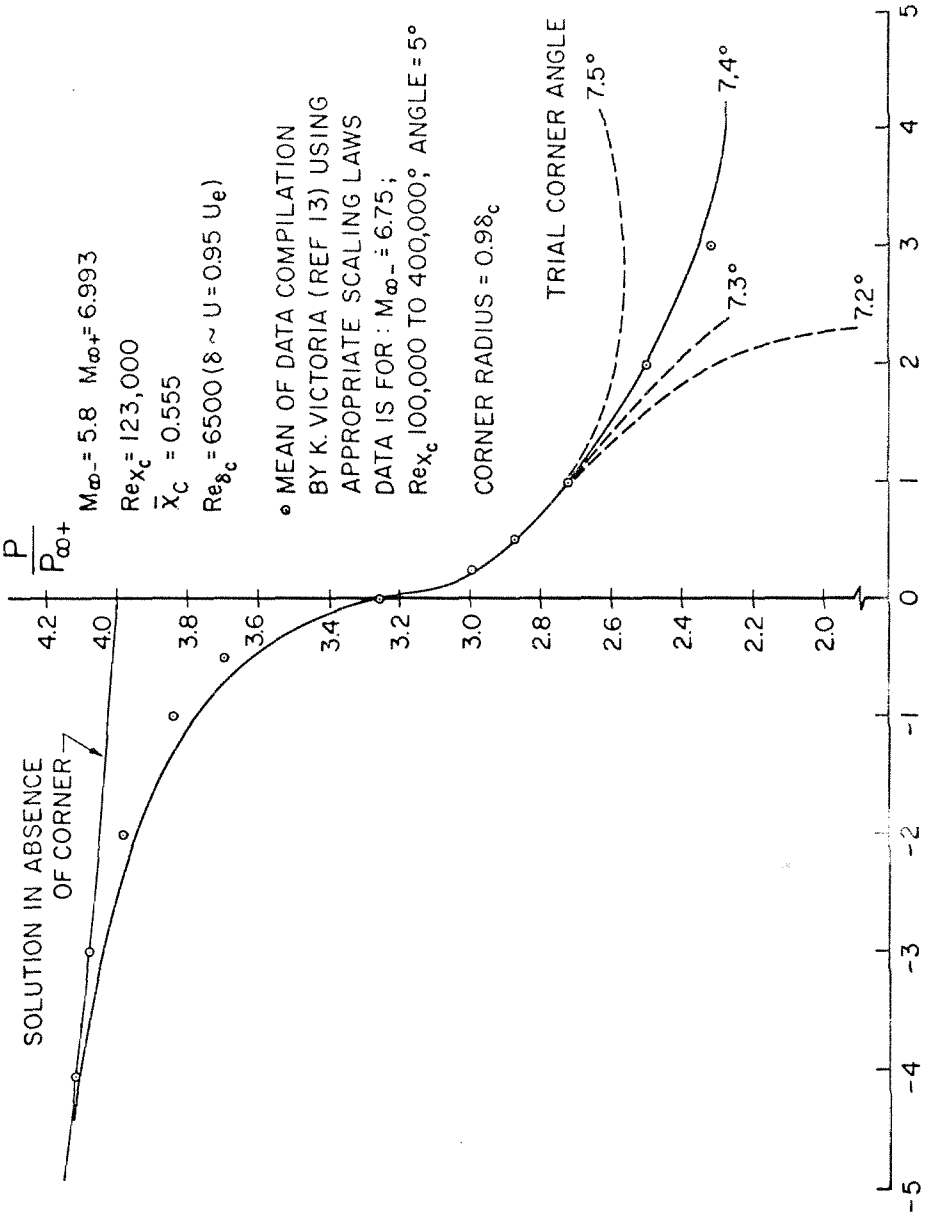

Fig. 26 EXPANSIVE CORNER PRESSURE DISTRIBUTION - FINITE DIFFERENCE METHOD

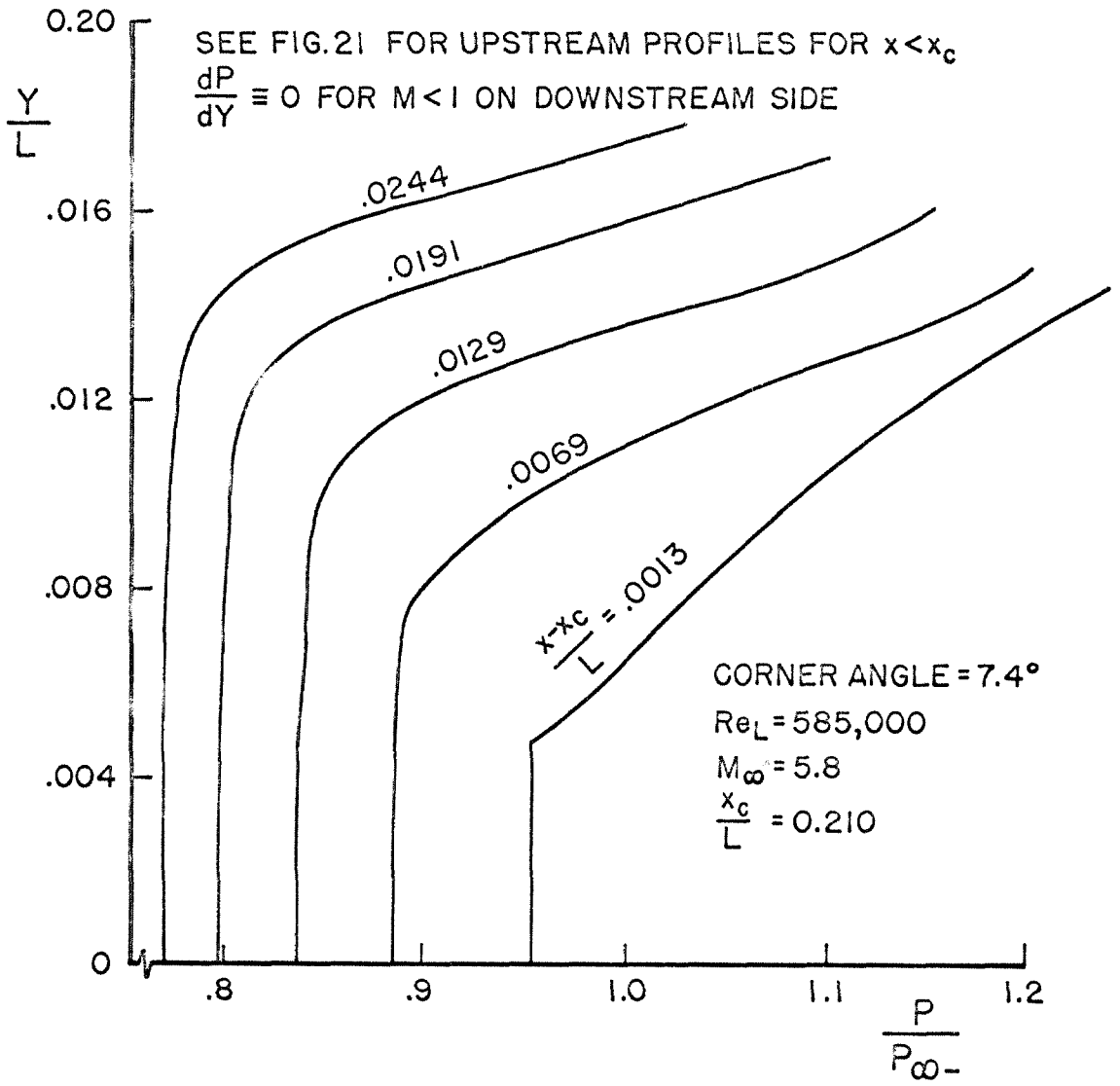

Fig. 27 PRESSURE PROFILES FOR EXPANSION CORNER-DOWNSTREAM SIDE

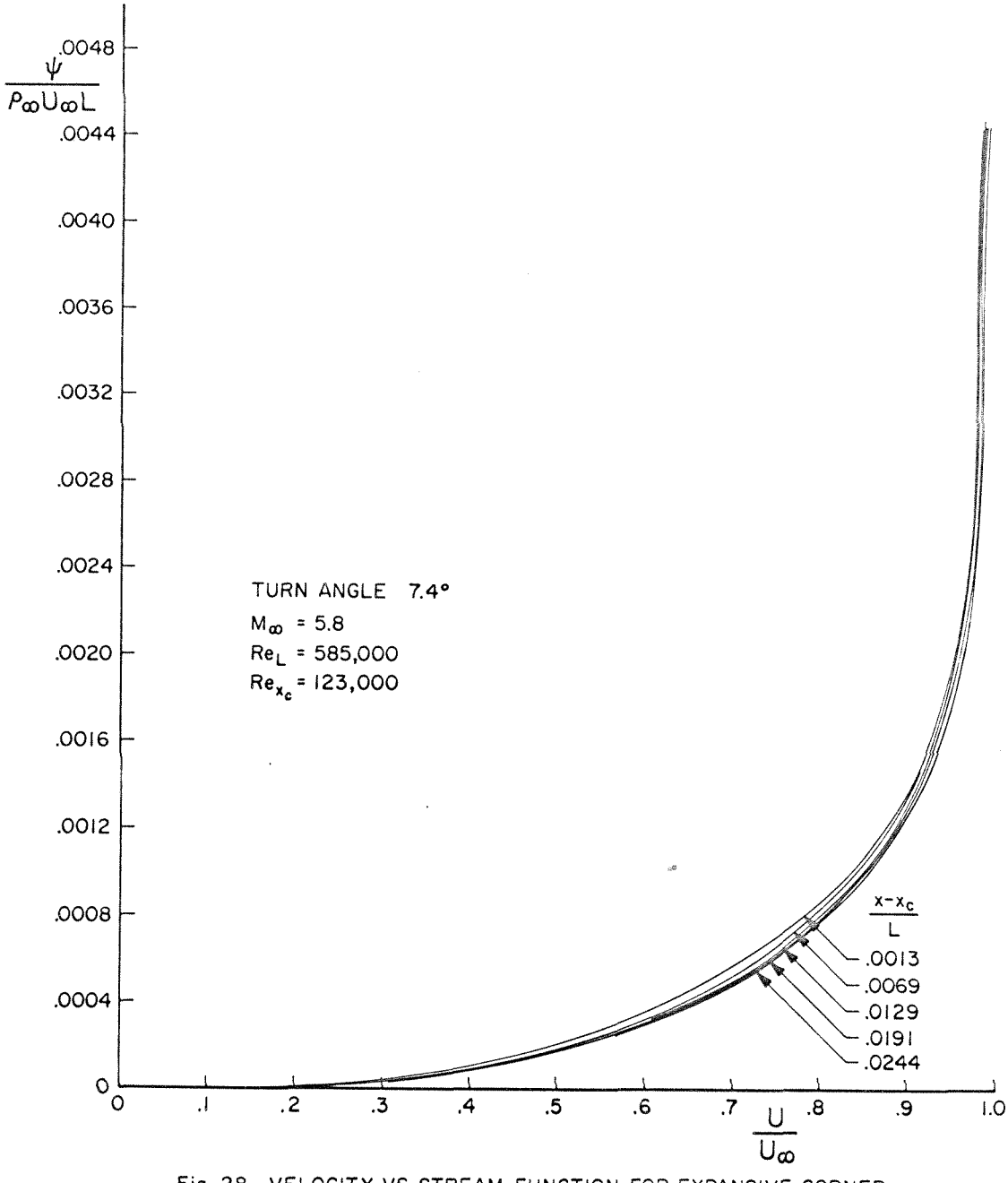

Fig. 28 VELOCITY VS. STREAM FUNCTION FOR EXPANSIVE CORNER

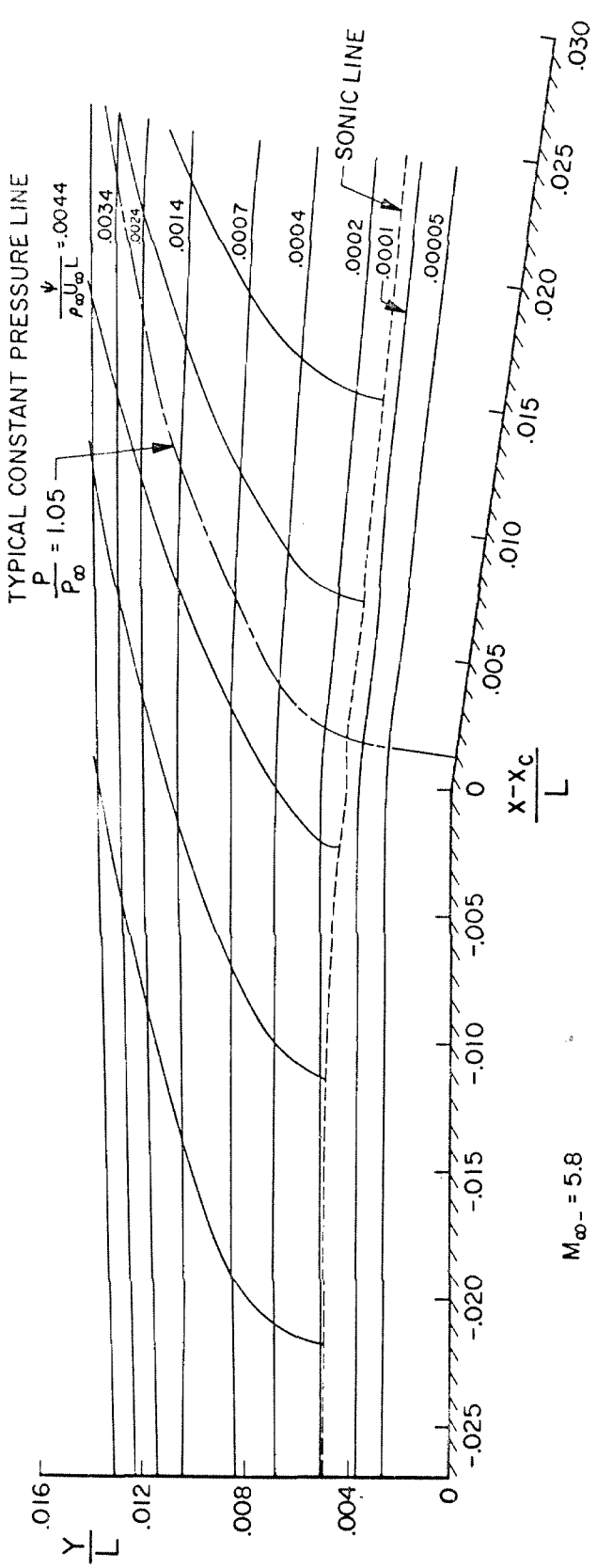

Fig. 29 EXPANSIVE CORNER STREAM LINE AND MACH LINE PATTERN

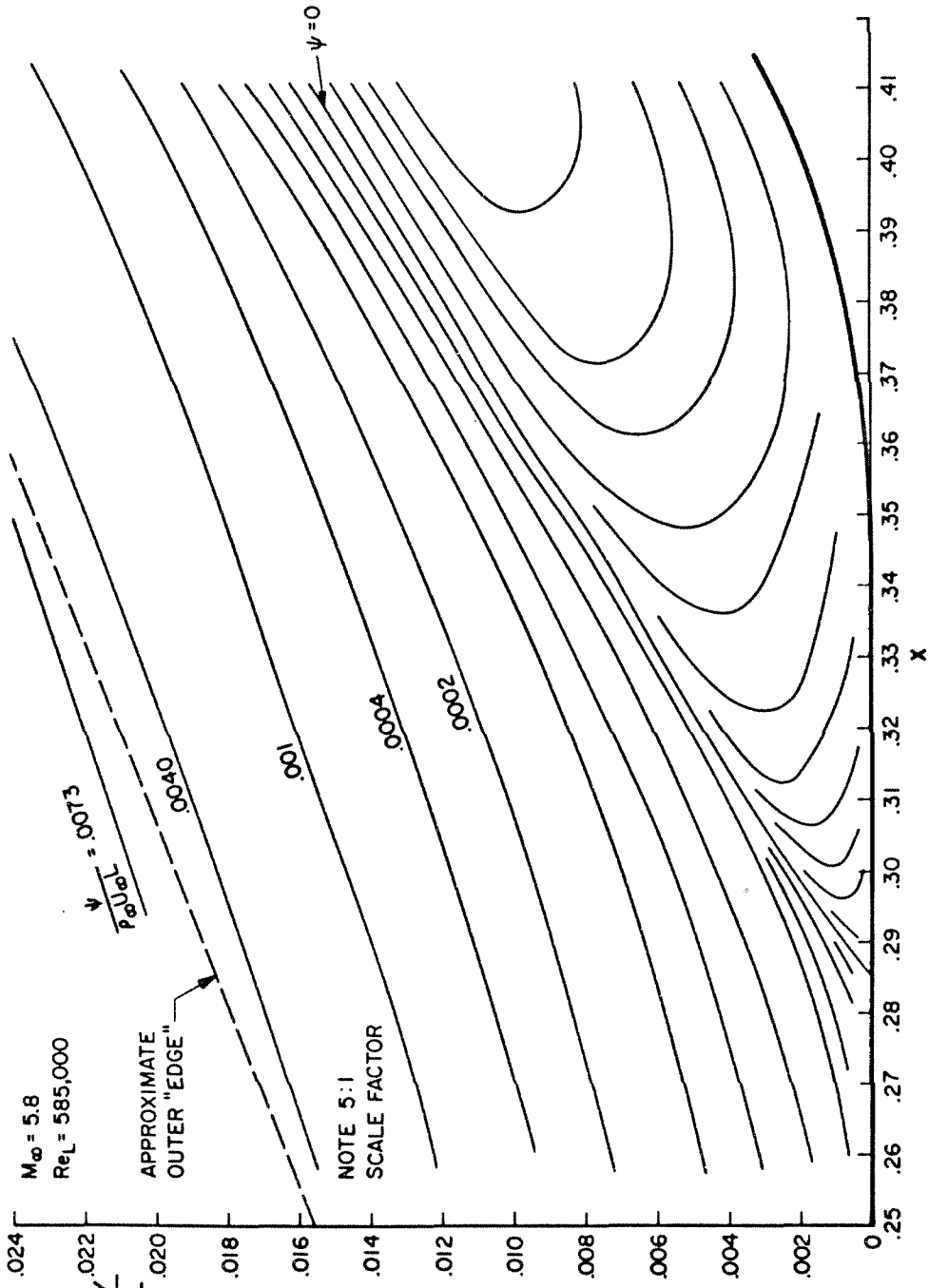

Fig. 30 COMPRESSION TURN STREAMLINE PATTERN

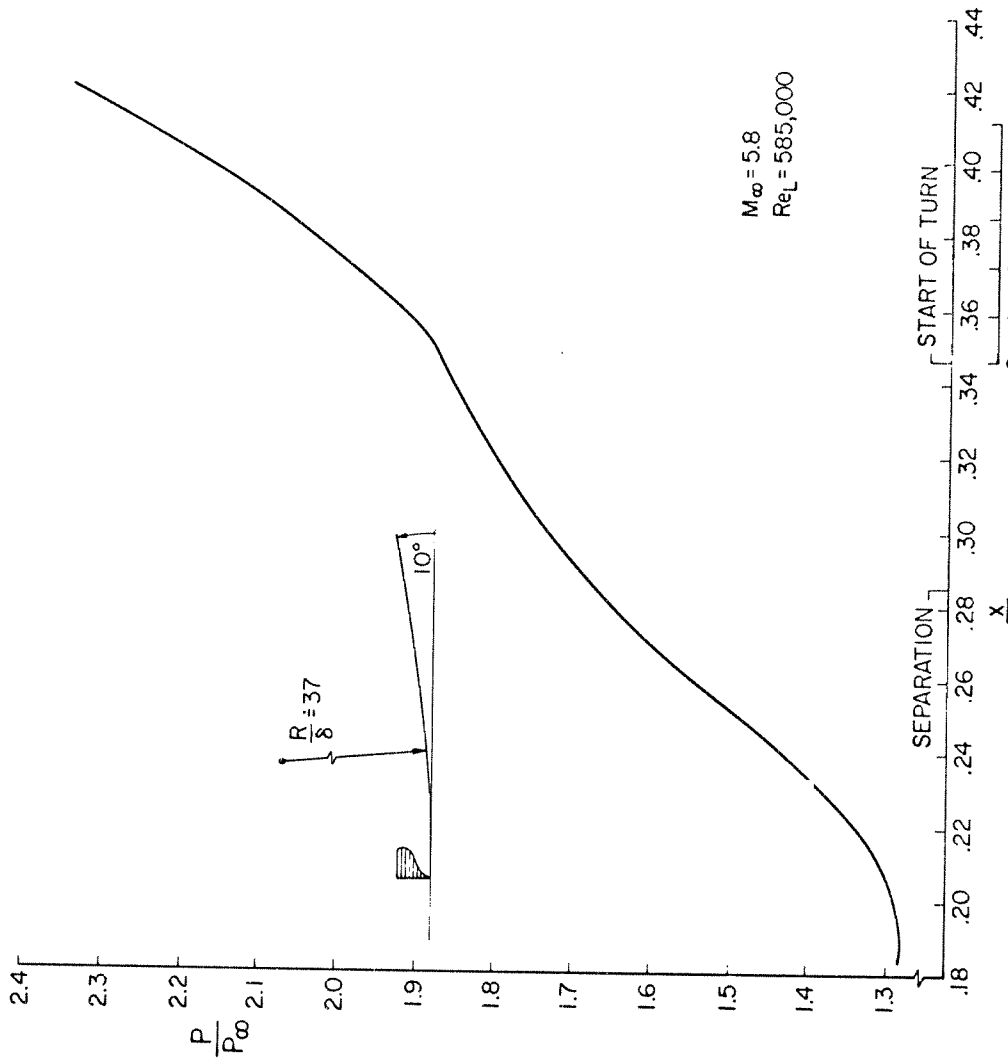

Fig. 31 INITIAL TRIAL FOR COMPRESSIVE CORNER SOLUTION

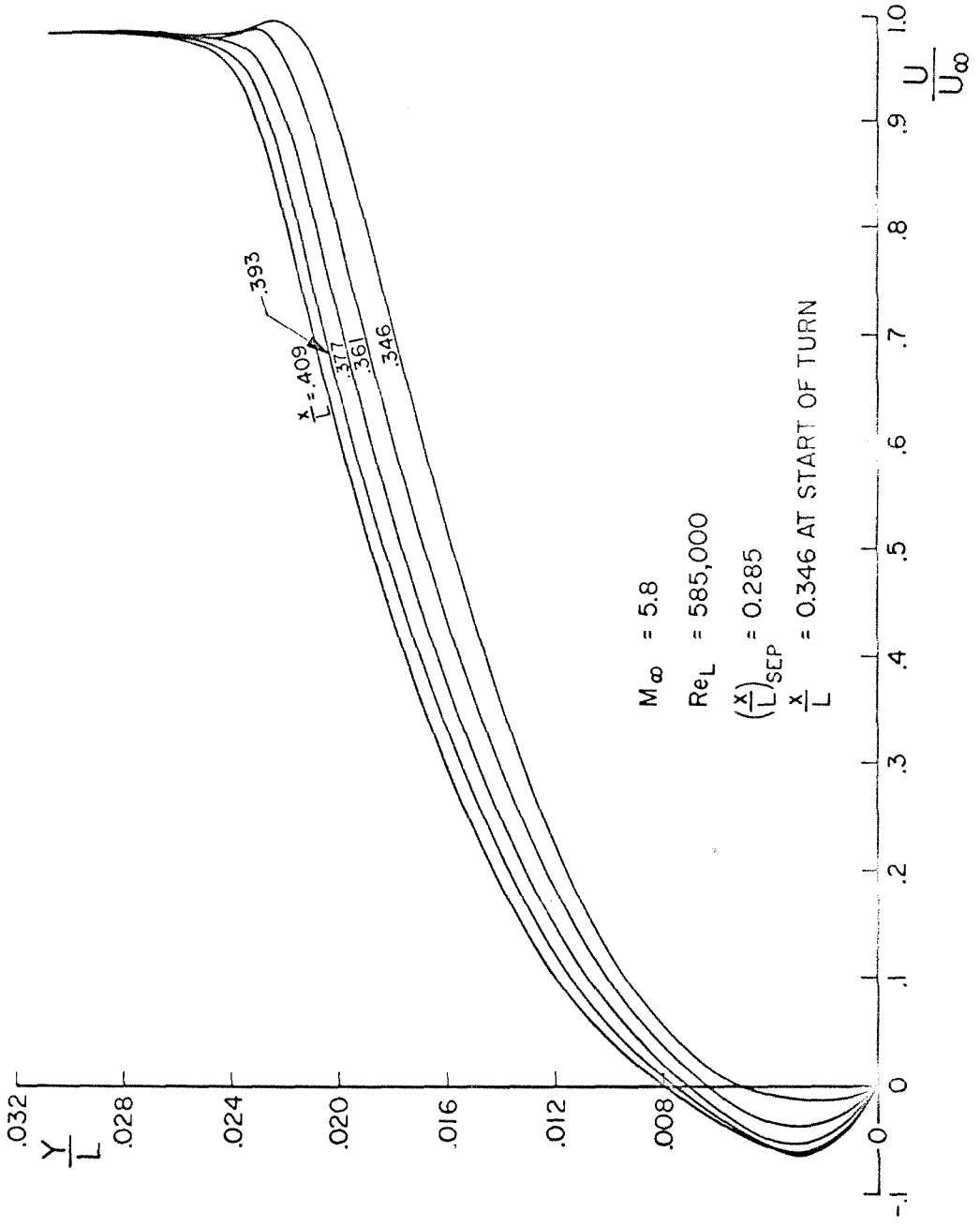

Fig. 32 U VELOCITY PROFILES-COMPRESSION TURN